Threshold pion photoproduction off nucleons using the nuclear model with explicit pions

Martin Mikkelsen
201706771

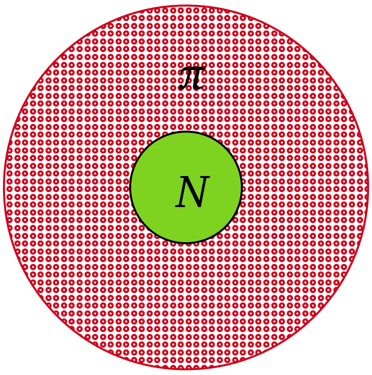

Master's thesis
Supervisor: Dmitri Fedorov

Department of Physics and Astronomy
Aarhus University
Denmark

November 2022

Summary

Lorem ipsum dolor sit amet, consectetuer adipiscing elit. Ut purus elit, vestibulum ut, placerat ac, adipiscing vitae, felis. Curabitur dictum gravida mauris. Nam arcu libero, nonummy eget, consectetuer id, vulputate a, magna. Donec vehicula augue eu neque. Pellentesque habitant morbi tristique senectus et netus et malesuada fames ac turpis egestas. Mauris ut leo. Cras viverra metus rhoncus sem. Nulla et lectus vestibulum urna fringilla ultrices. Phasellus eu tellus sit amet tortor gravida placerat. Integer sapien est, iaculis in, pretium quis, viverra ac, nunc. Praesent eget sem vel leo ultrices bibendum. Aenean faucibus. Morbi dolor nulla, malesuada eu, pulvinar at, mollis ac, nulla. Curabitur auctor semper nulla. Donec varius orci eget risus. Duis nibh mi, congue eu, accumsan eleifend, sagittis quis, diam. Duis eget orci sit amet orci dignissim rutrum.

Resumé

Lorem ipsum dolor sit amet, consectetuer adipiscing elit. Ut purus elit, vestibulum ut, placerat ac, adipiscing vitae, felis. Curabitur dictum gravida mauris. Nam arcu libero, nonummy eget, consectetuer id, vulputate a, magna. Donec vehicula augue eu neque. Pellentesque habitant morbi tristique senectus et netus et malesuada fames ac turpis egestas. Mauris ut leo. Cras viverra metus rhoncus sem. Nulla et lectus vestibulum urna fringilla ultrices. Phasellus eu tellus sit amet tortor gravida placerat. Integer sapien est, iaculis in, pretium quis, viverra ac, nunc. Praesent eget sem vel leo ultrices bibendum. Aenean faucibus. Morbi dolor nulla, malesuada eu, pulvinar at, mollis ac, nulla. Curabitur auctor semper nulla. Donec varius orci eget risus. Duis nibh mi, congue eu, accumsan eleifend, sagittis quis, diam. Duis eget orci sit amet orci dignissim rutrum.

Colophon

Threshold pion photoproduction off nucleons using the nuclear model with explicit pions

Master's thesis by Martin Mikkelsen

The project is supervised by Dmitri Fedorov

Typeset by the author using LaTeX and the memoir document class. Figures are made with the using the Seaborn package in Python and the Tikz package.

Code for document, figures and numerical calculations can be found on `https://github.com/MartinMikkelsen`

Printed at Aarhus University

Contents

Chapter 1

Introduction

Nuclear physics covers and expands different ideas from other areas of physics. These include but are not limited to low- and high-energy physics, few- and many-body dynamics, and classical and quantum statistical mechanics. Two concepts are needed when discussing nuclear physics: the nucleon and mesons. Nuclei consist of nucleons and are held together by the nuclear forces – by exchanging mediating quanta called mesons. This is similar to how the photon exchange generates the electromagnetic force. There are many different mesons, but the lightest mesons are called the pions (π^-, π^0, π^+) with a mass of about one-seventh of the nucleon leaving us in the MeV range. This energy scale also defines the regime known as low-energy physics, where the nucleus can be considered non-relativistic, and the mesons are virtual particles hidden in nucleon-nucleon interactions. Generally speaking, within the domain of low-energy nuclear physics, the nucleus appears as a self-bound many-body nucleonic system with intrinsic degrees of freedom. These systems are mesoscopic, along with atoms, molecules, micro- and nano-devices of condensed matter systems, and quantum computers. This means they are sufficiently large to have statistical regularities yet also small enough to study individual quantum states.

Increasing the energy will reveal the intermediate region of nuclear physics. Here relativistic effects become more important, and the meson and nucleon excitations become explicit. This energy scale is loosely characterised by an energy scale of a few GeV. At even higher energies and higher momentum transfer, dissecting the constituent of the nucleons and mesons is possible. These are known as quarks and gluons, and now the energy scale is in the TeV range. Generally speaking, the field of nuclear physics covers an energy range from KeV to TeV and the two different regimes of relativistic effects.

1.1 Strong Interactions

Using the uncertainty relation, one can estimate the range of the nuclear forces. If we assume the interaction is mediated by quanta being emitted by one particle and absorbed by another particle, we gain insight into two properties of the strong nuclear force. Firstly, the pion exchange as a mechanism for the nucleon interaction and secondly how the range of the strong nuclear force is characterised by the Compton wavelength of the lightest possible mediator. In the case of the neutral pion, this is approximately 1.46 fm.

1.2 Outline of Thesis

This thesis is organised as follows. Chapter 2 will cover the theoretical background needed for the other chapters. This includes how we can describe the interaction of radiation with matter within the framework of the 2nd quantization. This chapter also covers the density of states where the main results are two expressions, one in the relativistic limit and one in the non-relativistic limit. Chapter 3 will introduce the nuclear model with explicit mesons. We will go through how the nuclear model with explicit mesons will be constructed generally. Next we consider the case where the mesons are pions and look at how we can determine an equation of motion for the pion-nucleon system. We then focus specifically on the one-pion approximation, which is the most straightforward appearance of the nuclear model with explicit pions off protons. This is closely related to how we formulate the dressing of the proton and arrive at an equation of motion that is to be solved. This is the subject of section 3.4, where we explore the flexibility of this model. Specifically, this means we test different form factors and do a relativistic expansion to explore how this affects the solutions found in the previous section. Finally, we test how changing the operator to another operator found in effective field theory affects the system. In chapter 4, we explore pion photoproduction using the model with explicit pions and how this emerges naturally as a photodisintegration process. We consider the four possible reactions: two off the proton and two off the neutron. To calculate the matrix elements, we make a dipole approximation in section 4.1, and an exact approach follows this in section 4.2. We do fits to extract the parameters for the model and compare them to experimental data. Some of the thesis made it into an article [7].

Chapter 2

Theoretical background

2.1 Interaction of Radiation with Matter

In the following, we will derive the necessary equations describing how a quantized vector field interacts with matter within the framework of the second quantization. We will assume the final quantized form of the vector potential given by

$$\mathbf{A}(\mathbf{r},t) = \sum_{\mathbf{k},\lambda} \sqrt{\frac{2\pi\hbar c^2}{\omega_k V}} \left(a_{k,\lambda} \mathbf{e}_{\mathbf{k},\lambda} \mathrm{e}^{i(\mathbf{k}\cdot\mathbf{r}) - i\omega_k t} + a^\dagger_{\mathbf{k},\lambda} \mathbf{e}^*_{\mathbf{k},\lambda} \mathrm{e}^{-i(\mathbf{k}\cdot\mathbf{r}) + i\omega_k t} \right). \quad (2.1)$$

We now consider a non-relativistic system of charged particles interacting with the electromagnetic field. In this thesis, we will consider a two-particle system, but in this section, we generalize the results to any integer of particles denoted by the subscript i. The interaction will enable the system to emit and absorb photons. We start with the Hamiltonian describing the many-body system given by $H_0(\mathbf{r}_i, \mathbf{p_i})$ with no field. We introduce a field and do the following substitution

$$\mathbf{p}_i \rightarrow \mathbf{p}_i - \frac{e_i}{c}\mathbf{A}(\mathbf{r}_i), \quad (2.2)$$

where e_i is the charge of the i'th particle and c is the speed of light. This leads to a new Hamiltonian, which now depends on the field variables

$$H_0 \rightarrow H_0' = H_0\left(\mathbf{r}_i, \mathbf{p}_i - \frac{e_i}{c}\mathbf{A}(\mathbf{r}_i)\right) + \sum_i e_i \phi(\mathbf{r}_i), \quad (2.3)$$

where the last term in equation (2.3) is the potential energy. We now introduce the radiation gauge choice, which is purely conventional and any other choice of gauge will result in the same equations, albeit more difficult. The radiation gauge [9] is given by

$$\boldsymbol{\nabla} \cdot \mathbf{A} = \phi = 0, \quad (2.4)$$

and the non-relativistic Hamiltonian of the system describing the interaction with the radiation field is given by

$$H = \sum_i \frac{1}{2m_i}\left(\mathbf{p} - \frac{e_i}{c}\mathbf{A}(\mathbf{r}_i)\right)^2, \quad (2.5)$$

where $\mathbf{A}(\mathbf{r}_i)$ is equation (2.1) at point $\mathbf{r}_i$ and m_i is the mass of the i'th particle. We assumed the interaction between particles depends on their coordinates, so the minimal inclusion of the electromagnetic field affects only the kinetic part. This is a fair approximation in the non-relativistic limit and does not account for velocity-dependant interactions such as spin-orbit[1]. The electromagnetic interaction is relatively weak, and its strength is given by the fine structure constant, $\alpha = e^2/(\hbar c)$. Generally speaking, this interaction can be taken into account in the lowest non-vanishing order of perturbation theory. We expand (2.5) and keep only the linear terms

$$H^{(1)} = -\sum_i \frac{e_i}{2m_i c}(\mathbf{p}_i \cdot \mathbf{A}(\mathbf{r}_i) + \mathbf{A}(\mathbf{r}_i) \cdot \mathbf{p}_i), \tag{2.6}$$

where the (1) represents the first non-vanishing order. Due to our choice of gauge equation (2.4) the two terms in (2.6) commute and we are left with

$$H^{(1)} = -\sum_i \frac{e_i}{m_i c}\mathbf{A}(\mathbf{r}_i, t) \cdot \mathbf{p}_i. \tag{2.7}$$

For the type of problems, we will be solving in chapter 4, we will be working mainly with a single charged particle, and we can ignore the sum in (2.7).

1. One could add a spin-orbit term to the non-relativistic approach, but this is not necessary for our calculations later.

2.2 Density of States

As mentioned in section 2.1 the electromagnetic interaction strength is related to the fine structure constant. In chapter 4, we want to do perturbation theory to get an expression for the total cross-section as a function of energy which the relatively weak fine structure constant allows. From perturbation theory, the transition rate is described by Fermi's golden rule given by

$$\mathrm{d}\omega = \frac{2\pi}{\hbar}|\mathcal{M}|^2 \,\mathrm{d}\rho, \tag{2.8}$$

where the matrix element $\mathcal{M}$ is the subject in chapter 4 and $\mathrm{d}\rho$ is the density of states in the final states. In this section, we will derive general results of the density of states in the non-relativistic and relativistic limits. The density of states is defined by

$$\rho(E) = \frac{\mathrm{d}n(E)}{\mathrm{d}E}, \tag{2.9}$$

where $n(E)$ is the number of states with energy E. Consider the number of states within the momentum space volume

$$\mathrm{d}^3\mathbf{p} = p^2 \mathrm{d}p \,\mathrm{d}\Omega_q, \tag{2.10}$$

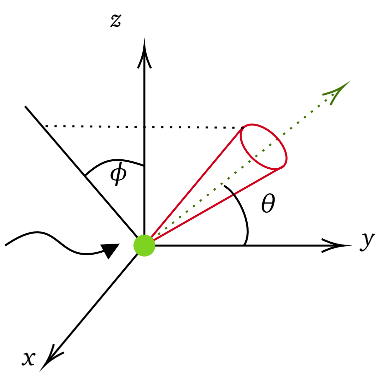

Figure 2.1: Differential cross section and the solid angle Ω_q (red cone).

where the subscript q is used to empathize momentum space. We will use this notation throughout the thesis[2]. Equation (2.10) corresponds to the momenta with magnitude from p to $p + \mathrm{d}p$ and within a cone of solid angle $\mathrm{d}\Omega_q$. This is illustrated in figure 2.1. We use that the solutions to the Schrödinger equation for a particle confined in a large volume with periodic boundary conditions are travelling waves. This leads to the following expression

$$\rho(p)\,\mathrm{d}\rho = \left(\frac{L}{2\pi\hbar}\right)^3 \mathrm{d}^3\mathbf{p} = \frac{V}{(2\pi\hbar)^3} p^2 \,\mathrm{d}p \,\mathrm{d}\Omega_q. \tag{2.11}$$

In chapter 4, we are interested in the number of possible final states with energy in the range between E_f and $E_f + \mathrm{d}E_f$ so we express (2.11) in terms of energy. This is given by

$$\rho(E_f) = \frac{V p_f^2}{(2\pi\hbar)^3} \frac{\mathrm{d}p_f}{\mathrm{d}E_f} \,\mathrm{d}\Omega_q. \tag{2.12}$$

2. The q might seem odd but in chapter 4 we will write the momentum as $\hbar\mathbf{q}$, where $\mathbf{q}$ is a wave number.

This is the final non-relativistic expression. However, we want to generalize this result to account for relativistic effects. For a general pion photoproduction process, we can write

$$N + \gamma \rightarrow N + \pi, \tag{2.13}$$

where N is the nucleon and γ is a photon. The final state energy [10] is then given by

$$E_f = E_N + E_\pi = \sqrt{p_f^2 c^2 + m_N^2 c^4} + \sqrt{p_f^2 c^2 + m_\pi^2 c^4}. \tag{2.14}$$

We now change the notation to match the variables used later in chapter 4 and write the final state momentum p_f in terms of the pion-nucleon wave number q.

From conservation of energy, we get the following expression for the energy of the relative pion-nucleon motion denoted E_q.

$$E_q = \sqrt{m_N^2 c^4 + (\hbar c)^2 q^2} + \sqrt{m_\pi c^4 + (\hbar c)^2 q^2} - m_N c^2 - m_\pi c^2. \tag{2.15}$$

Looking at (2.12), we want to get an expression for the final state momentum in terms of the wave number. The density of states around $\mathbf{q}$ is given by

$$\mathrm{d}\rho_f = \frac{Vq}{(2\pi)^3} \frac{1}{2} \frac{\mathrm{d}q^2}{\mathrm{d}E_q} \mathrm{d}\Omega_q. \tag{2.16}$$

We now solve for $(\hbar c)^2 q^2$ in (2.15), which yields the following result[3]

$$(\hbar c)^2 q^2 = \frac{E_q(E_q + 2m_N c^2)(E_q + 2m\pi c^2)(E_q + 2m_N c^2 + 2m_\pi c^2)}{4(E_q + m_N c^2 + m_\pi c^2)^2}, \tag{2.17}$$

and we are now able to calculate the derivative of equation (2.17)

$$\begin{aligned}(\hbar c)^2 \frac{\mathrm{d}q^2}{\mathrm{d}E_q} &= \frac{(E_q^2 + 2E_q m_N c^2 + 2m_N^2 c^4 + 2E_q m_\pi c^2 + 2m_N m_\pi c^4)}{2(E_q + m_N c^2 + m_\pi c^2)^3} \\ &\quad \times \frac{(E_q^2 + 2E_q m_N c^2 + 2m_\pi^2 c^4 + 2E_q m_\pi c^2 + 2m_N m_\pi c^4)}{2(E_q + m_N c^2 + m_\pi c^2)^3},\end{aligned} \tag{2.18}$$

which yields the final expression for the relativistic density of states by plugging equation (2.18) into equation (2.16). Non-relativistically, the density of states in terms of E_q and q is given by the following using

$$\mathrm{d}\rho_f = \frac{Vq\mu_{N_\pi}}{(2\pi)^3 \hbar^2} \mathrm{d}\,\Omega_q. \tag{2.19}$$

We now have to expressions for the density of states to use in conjunction with equation (2.8). In chapter 4 we will refer to equation (2.18) as the relativistic density of states and equation (2.19) as the non-relativistic density of states.

3. It is also possible to use the approximation that $\sqrt{x^2 + y^2} \simeq 0.96x + 0.4y$ giving an error of only 4%.

Chapter **3**

The Nuclear Model with Explicit Mesons

We consider a nuclear model where the nucleus is held together by emitting and absorbing mesons, and the mesons are treated explicitly [6]. We are considering the regime of low-energy nuclear physics, and this model is different from conventional interaction models in several ways. Firstly, the nucleons interact by emitting and absorbing mesons, not via a phenomenological potential. Conceptually this is similar to the one-boson-exchange model. Secondly, the number of parameters is greatly reduced. Regardless of the meson type, the number of parameters is two; the range and the strength of the meson-nucleon coupling are denoted b and S, respectively. In the case of the pion, the central force, tensor force and the three-body force are all concealed within these two parameters. This model should be able to reproduce phenomena within the realm of low-energy nuclear physics, such as the deuteron, nucleon-nucleon scattering, pion-nucleon scattering and pion photoproduction. The low energy regime also enables the use of the Schrödinger equation to describe the equations of motion. The model must be constructed in a way such that usual quantum numbers are conserved; this means conservation of isospin, angular momentum and parity.

3.1 Nuclear Interacting Model with Explicit Pions

In the following, we focus on the nuclear model with explicit pions [5]. The pion is the lightest of the strongly interacting particles with a mass of about 15% of the nucleon mass. This yields a large Compton wavelength of 1.4 fm, which provides the longest-ranged contribution to the nucleon-nucleon interaction [11]. Furthermore, the pion is a significant component of the nuclear wave function where the pion dominates meson exchange corrections to different nuclear properties. In general, the bare nucleon is surrounded by several virtual pions. They are virtual in the same sense that the positron-electron pair are virtual in pair creation from a photon. It is important to stress that these are virtual since they can have properties impossible for real particles. The multi-component wave function of the nucleon can be written as

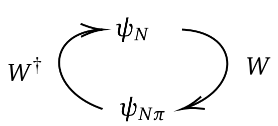

Figure 3.1: Illustration of the pion-nucleon operator, W

$$\Psi_N = \begin{bmatrix} \psi_N \\ \psi_{N\pi} \\ \psi_{N\pi\pi} \\ \vdots \end{bmatrix}, \tag{3.1}$$

where ψ_N is the bare nucleon, and the other wave functions are dressed by an arbitrary number of pions indicated by the subscripts. Assuming the nuclear interaction conserves isospin, angular momentum and parity, we can construct the following operator for the pion-nucleon operator [14]

$$W \equiv (\boldsymbol{\tau} \cdot \boldsymbol{\pi})(\boldsymbol{\sigma} \cdot \mathbf{r}) f(r) \tag{3.2}$$

$$W^\dagger \equiv \int_V \mathrm{d}^3 r \, (\boldsymbol{\tau} \cdot \boldsymbol{\pi})^\dagger (\boldsymbol{\sigma} \cdot \mathbf{r})^\dagger f(r), \tag{3.3}$$

where $\boldsymbol{\tau}$ is the isovector of Pauli matrices acting on the nucleon in isospin space and $\boldsymbol{\sigma}$ is the same but for spin space and $\mathbf{r}$ is the relative coordinate distance between the nucleon and the pion. Note that the $W^\dagger$ operator contains an integral to remove the coordinate of the annihilated pion. These operators ensure the conservation of isospin, angular momentum and parity. The isovector of pions is denoted $\boldsymbol{\pi}$ and can be combined with $\boldsymbol{\tau}$ and be represented as a 2-by-2 hermitian matrix [15] given by

$$\boldsymbol{\tau} \cdot \boldsymbol{\pi} = \tau_0 \pi_0 + \sqrt{2}\tau_- \pi^+ \sqrt{2}\tau_+ \pi^- = \begin{bmatrix} \pi^0 & \sqrt{2}\pi^- \\ \sqrt{2}\pi^+ & -\pi^0 \end{bmatrix}, \tag{3.4}$$

where the isospin coefficients will be important later when we discuss different photoproduction processes. Similarly, by expanding the matrices in spin space and using the spherical tensor operator, we get the following matrix in terms of the spherical harmonics

$$\boldsymbol{\sigma} \cdot \mathbf{r} = \sqrt{\frac{4\pi}{3}} r \begin{bmatrix} Y_1^0 & \sqrt{2} Y_1^{-1} \\ \sqrt{2} Y_1^1 & Y_1^0 \end{bmatrix}, \tag{3.5}$$

where similar to in isospin space, the off-diagonals include a factor $\sqrt{2}$.

There is also a phenomenological, short-range form factor $f(r)$ given by

$$f(r) = \frac{S}{b} \mathrm{e}^{-r^2/b^2}, \tag{3.6}$$

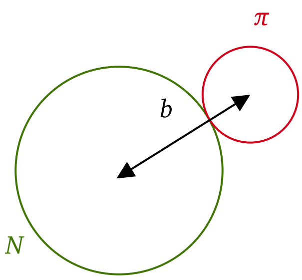

Figure 3.2: Schematic figure of the system to describe the form factor, (3.6). The pion is assumed to sit on the surface.

where S and b are the pion-nucleon coupling strength and range, respectively. These are illustrated in figure 3.2. The action of annihilating a pion must include the integral over coordinate space to remove the coordinate. We now have everything we need to construct a general Hamiltonian for the multi-component wave function of the nucleon in (3.1)

$$H = \begin{bmatrix} K_N & W^\dagger & 0 & \dots \\ W & K_N + K_\pi + m_\pi c^2 + V_C & W^\dagger & \dots \\ 0 & W & K_N + K_{\pi(1)} + K_{\pi(2)} + 2m_\pi c^2 + V_C & \dots \\ \vdots & \vdots & \vdots & \ddots \end{bmatrix}, \tag{3.7}$$

where the kinetic operators are given by

$$K_N = \frac{-\hbar^2}{2m_N c^2} \frac{\partial}{\partial \mathbf{R}^2} \tag{3.8}$$

$$K_\pi = \frac{-\hbar^2}{2m_\pi c^2} \frac{\partial}{\partial \mathbf{r}^2}. \tag{3.9}$$

Note the different derivatives–here $\mathbf{R}$ is the centre-of-mass coordinate, and $\mathbf{r}$ is the relative coordinate. The subscripts on the kinetic operators in (3.7) represent the order in which the pions are created. Should there be charged particles involved, one must include a Coulomb interaction denoted by V_C. From (3.1) and (3.7) we can construct the general Schrödinger equation

$$H\Psi_N = E\Psi_N, \tag{3.10}$$

where the ground state is the bare nucleon surrounded by virtual pions. The ground state energy in the rest frame of the nucleon gives the mass of the physical nucleon. Within the framework of this model, one can generate a physical pion by supplying enough energy such that the pion is no longer virtual. The pion is trapped behind a potential barrier of height $m_\pi c^2 = 140$ MeV and cannot leave unless this or more energy is supplied to the system. This is illustrated on figure 3.3.

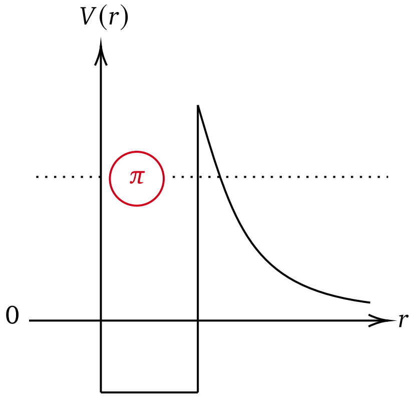

Figure 3.3: Illustration of the virtual pion

3.2 Dressing of the Nucleon in the One Pion Approximation

We now consider the scenario where a photon interacts with the nucleon-pion systems and generates a physical pion. This means the energy is higher than the potential barrier also when taking recoil effects into account. This also hints at how a pion photoproduction process would emerge naturally as a disintegration process in this nuclear model. To generate more pions, the photon energy would have to be increased by the same amount. This also means that the first pion is responsible for the largest contribution to the nucleon dressing. This will be referred to as the one-pion approximation. As a proof-of-concept, we constrain ourselves to the one pion approximation and adding more pions should, in principle, be a straightforward extension of the following calculations.

Returning to (3.1) and enforcing the one-pion approximation yields

$$\Psi = \begin{bmatrix} \psi_N(\mathbf{R}) \\ \psi_{N\pi}(\mathbf{r}) \end{bmatrix}. \tag{3.11}$$

The Hamiltonian, which acts on the two-component wave function in (3.11) is given by[1]

$$H = \begin{bmatrix} K_N & W^\dagger \\ W & K_N + K_\pi + m_\pi c^2 \end{bmatrix}, \tag{3.12}$$

1. Strictly speaking, one should use a three-component wave function to account for the mass difference between π^0 and $\pi^\pm$. This is done in appendix C. This shows no noticeable difference.

So far we have kept the model as simple as possible by expressing the equations in terms of the nucleon. From now on, we treat the nucleon of two states of the same strongly interacting object with an intrinsic degree of freedom which defines the proton and neutron. We choose the proton and neutron as

$$|p\rangle = \begin{bmatrix} 1 \\ 0 \end{bmatrix} \quad |n\rangle = \begin{bmatrix} 0 \\ 1 \end{bmatrix}. \tag{3.13}$$

Furthermore, we denote the spin state of the nucleon by an arrow

$$|\uparrow\rangle = \begin{bmatrix} 1 \\ 0 \end{bmatrix} \quad |\downarrow\rangle = \begin{bmatrix} 0 \\ 1 \end{bmatrix}. \tag{3.14}$$

The wave function must also be normalised to one nucleon per unit volume. This is as far as we get in general terms for the dressing of the nucleon in the one-pion approximation.

3.3 Dressing of the Proton

We now focus our attention on the dressing of the proton in the spin-up state. The calculations are almost identical, remembering the definitions from section 3.2. The wave function of the bare proton can thus be written as

$$\psi_p = \frac{p\uparrow}{\sqrt{V}}, \tag{3.15}$$

where we omit the kets to unclutter the notation. The Hamiltonian (3.12) suggest the following expression for the wave function of the pion-nucleon system

$$\psi_{N\pi} = (\boldsymbol{\tau}\cdot\boldsymbol{\pi})(\boldsymbol{\sigma}\cdot\mathbf{r})\frac{p\uparrow}{\sqrt{V}}\phi(r), \tag{3.16}$$

where $\phi(r)$ is the wave function which will play an integral part in the rest of this section. From (3.2), we can construct the Schrödinger equation of the system

$$\begin{bmatrix} K_p & W^\dagger \\ W & K_N + K_\pi + m_\pi c^2 \end{bmatrix}\begin{bmatrix} \psi_p \\ \psi_{N\pi} \end{bmatrix} = E\begin{bmatrix} \psi_p \\ \psi_{N\pi} \end{bmatrix}. \tag{3.17}$$

Note that the kinetic operator in the second row still contains K_N to emphasise that this acts on the general nucleon-pion wave function, $\psi_{N\pi}$. Expanding (3.17) yields two equations

$$K_p\psi_p + W^\dagger\psi_{N\pi} = E\psi_p \tag{3.18}$$

$$W\psi_p + (K_N + K_\pi + m_\pi c^2)\psi_{N\pi} = E\psi_{N\pi}. \tag{3.19}$$

In the rest frame of the proton, the center-of-mass dependency vanishes and inserting the operator (3.2) yields

$$\int_V \mathrm{d}^3r\,(\boldsymbol{\tau}\cdot\boldsymbol{\pi})^\dagger(\boldsymbol{\sigma}\cdot\mathbf{r})^\dagger f(r)\phi(r)(\boldsymbol{\tau}\cdot\boldsymbol{\pi})(\boldsymbol{\sigma}\cdot\mathbf{r})p\frac{1}{\sqrt{V}} = Ep\frac{1}{\sqrt{V}}, \tag{3.20}$$

where the integration comes from equation (3.3). This can be further simplified using relations for the matrix vectors[2]

$$12\pi\int_0^\infty \mathrm{d}r\, f(r)\phi(r)r^4 = E. \tag{3.21}$$

2. $(\boldsymbol{\tau}\cdot\boldsymbol{\pi})^\dagger(\boldsymbol{\tau}\cdot\boldsymbol{\pi}) = 3$ and $(\boldsymbol{\sigma}\cdot\mathbf{r})^\dagger(\boldsymbol{\sigma}\cdot\mathbf{r}) = r^2$

Similarly for (3.19) where the term $K_N\psi_{N\pi}$ vanishes,

$$\begin{aligned}(\boldsymbol{\tau}\cdot\boldsymbol{\pi})(\boldsymbol{\sigma}\cdot\mathbf{r})f(r)p\frac{1}{\sqrt{V}} - \frac{\hbar^2}{2\mu_{N\pi}}\nabla^2_{\mathbf{r}}(\boldsymbol{\tau}\cdot\boldsymbol{\pi})(\boldsymbol{\sigma}\cdot\mathbf{r})p\frac{1}{\sqrt{V}}\phi(r) \\ = (E - m_\pi c^2)(\boldsymbol{\tau}\cdot\boldsymbol{\pi})(\boldsymbol{\sigma}\cdot\mathbf{r})\phi(r)p\frac{1}{\sqrt{V}},\end{aligned} \tag{3.22}$$

using (3.9) and where $\mu_{N\pi}$ is the reduced mass of the nucleon-pion system. This equation can be further simplified by using a vector operator relation which yields[3]

3. $\nabla^2(\mathbf{r}\phi(r)) = \mathbf{r}\left(\frac{\mathrm{d}^2\phi(r)}{\mathrm{d}r^2} + \frac{4}{r}\frac{\mathrm{d}\phi(r)}{\mathrm{d}r}\right)$

$$f(r) - \frac{\hbar^2}{2\mu_{N\pi}}\left(\frac{\mathrm{d}^2\phi(r)}{\mathrm{d}r^2} + \frac{4}{r}\frac{\mathrm{d}\phi(r)}{\mathrm{d}r}\right) = (E - m_\pi c^2)\phi(r). \tag{3.23}$$

This means equation (3.21) and (3.23) are the two equations that must be solved numerically.

$$\left.\begin{aligned} &12\pi\textstyle\int_0^\infty \mathrm{d}r\, f(r)\phi(r)r^4 = E \\ &f(r) - \tfrac{\hbar^2}{2\mu_{N\pi}}\left(\tfrac{\mathrm{d}^2\phi(r)}{\mathrm{d}r^2} + \tfrac{4}{r}\tfrac{\mathrm{d}\phi(r)}{\mathrm{d}r}\right) + m_\pi c^2\phi(r) = E\phi(r)\end{aligned}\right\} \tag{3.24}$$

The bracket on the right is used to empathise that (3.24) is a coupled system.

3.4 Numerical Considerations

To solve the system of equations (3.24), one can consider two different numerical approaches. One approach gives a more intuitive picture of how to solve this equation, while the other is more robust and practical.

For a given E, one can solve the second-order differential equation corresponding to $\phi(E)$. Conversely, for a given $\phi(r)$, one can calculate the integral to find $E(\phi)$. This leads to the fixed-point equation given by

$$E(\phi(\mathcal{E})) = \mathcal{E}, \tag{3.25}$$

which is a single variable non-linear equation. Equation (3.25) can be solved using a root-finding algorithm. This approach is generally not as efficient since the algorithm will have to search through large parameter space to find a suitable solution.

The second approach consists of reformulating the system (3.24) as a boundary value problem with the following conditions

$$I'(r) = 12\pi f(r)\phi(r)r^4, \quad I(0) = 0,\ I(\infty) = E, \tag{3.26}$$

where I is the integral in equation (3.24). Essentially, the boundary conditions we require for the energy are written in equation (3.26). The equation starts from a singular point and extends to infinity. We require the solution to stay finite, which means approximations are needed at both limits. At $r \longrightarrow 0$, the differential equation is approximately an Euler-Cauchy equation with basis solutions 1 and r^{-1}. For finite solutions, the latter is ignored which means $\phi'(a) = 0$ is the requirement for $a \approx 0$.[4] For $r \longrightarrow \infty$, the dominating term in the differential equation is

4. You would end up with the same conclusion if you consider $\phi = a + r^n$ and plug this into $\phi'' + 4\phi'/r = 0$, which yields $n = 0, -1$.

$$-\phi''(r) + 2\mu_{N\pi}(m_\pi c^2 - E)\phi(r) = 0. \tag{3.27}$$

Since we expect a negative value for E, the basis solutions are on the form

$$\phi(r) = \exp\left\{\pm\sqrt{2\mu_{N\pi}(m_\pi c^2 + |E|)}\right\}r. \tag{3.28}$$

In the case of a positive sign, the solution diverges. For the basis solution with negative exponents, we have

$$\phi'(r) + \sqrt{2\mu_{N\pi}(m_\pi c^2 + |E|)}\phi(r) = 0. \tag{3.29}$$

These two conditions are suitable boundary conditions for the left and right boundaries, respectively. The algorithm converges, and a solution to (3.17) is found. The solutions can be seen in figure 3.4 for the parameters $S = 10$ MeV and $b = 1$ fm.

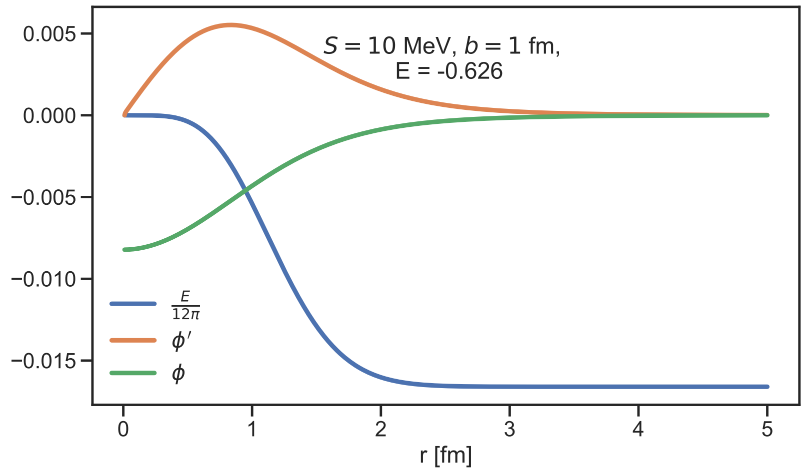

Figure 3.4: Boundary value problem solutions. The blue line representing the energy is scaled.

Also, note that since we expect the energy to be less than zero, it makes sense for the wave function to be negative since all other terms in the integral in equation (3.24) are positive. It might appear strange to have a negative wave function, $\phi(r)$, but there are two things to note. One can add an arbitrary phase to equation (3.11) and flip the sign. Also, for all calculations, we are only interested in the norm-square of the wave function. The energy for the parameters shown in figure 3.4 is $E = -0.626\,\text{MeV}$ and this value is very sensitive to the parameters S and b since they enter in the form factor as seen in equation (3.6) and as mentioned in section 3.1 this gives the physical mass of the proton–it's importance will be clear later when comparing the discussion the mass contribution from virtual pion in chapter 4.

Since we cannot allow the wave function to extend to infinity numerically, we must introduce some cut-off. Since the wave function of the pion-nucleon system has a built-in range parameter b, it is natural to let the cut-off be proportional to this parameter. Within the regime of nuclear physics, we expect the wave function to extend up to a length within the order of magnitude of ten fermi. Quantitatively this means a small constant of proportionality in front of r_{min} and another constant in front of r_{max}. Numerically, a constant of proportionality for r_{max} and the impact can be seen in figure 3.5 where the radial wave functions stop after $5r_{\text{max}}$.

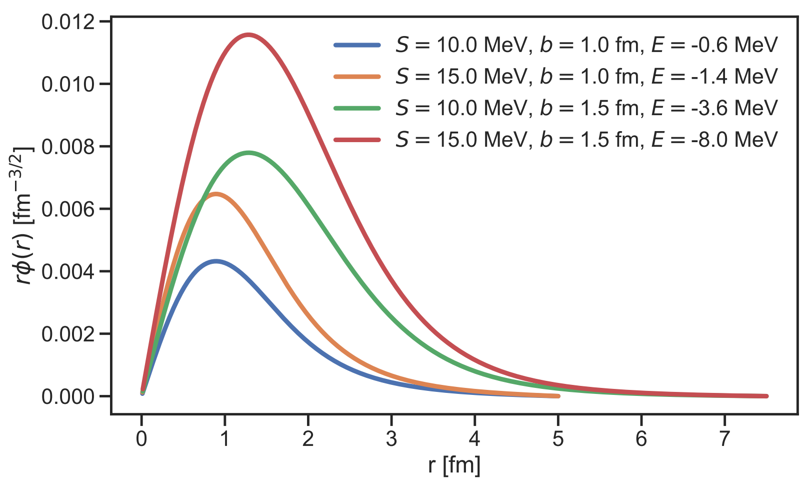

Figure 3.5: Radial wave function for different parameters S and b to illustrate the behavoir on the radial function.

Figure 3.5 also illustrates the behaviour of the radial wave functions as the parameters change. As the coupling strength parameter S increases, the radial wave function increases. As the range parameter b increases, the peak is shifted to this new value. Also, note the unit of the radial wave function. We know the following integral must be dimensionless

$$\int_V \mathrm{d}^3R \int_V \mathrm{d}^3r \,|\, \psi_{N\pi}|^2 \,, \tag{3.30}$$

which means the wave function $\phi(r)$ must have dimensions of $\text{fm}^{-5/2}$, and the radial wave function $r\phi(r)$ must have dimensions of $\text{fm}^{-3/2}$. Note here the two integrals come from the annihilation of a pion and the normalisation of one particle per unit volume, respectively.

3.4.1 Different Form Factors

Compared to conventional interaction models of the nucleus, this model has the advantage of having very few parameters. The phenomenological form factor $f(r)$ only consists of an interaction strength S and a range parameter b. The form factor can take many forms, yielding different wave function solutions and changing the energy. The formalism in section 3.4 is very flexible to changes in the form factor, and here we explore how different form factors impact the wave function. The form factors must all decrease as a function of r since we constrain the system to short-range forces. The solutions in figure 3.5 assume the form factor from equation (3.6), which is Gaussian. A priori, we do now know anything about the form factor, and it might as well be Yukawa like

$$f(r) = \frac{S}{b} \frac{\exp\left\{-\frac{r}{b}\right\}}{r}. \tag{3.31}$$

Figure 3.6 shows the radial wave functions if the form factor is Yukawa like

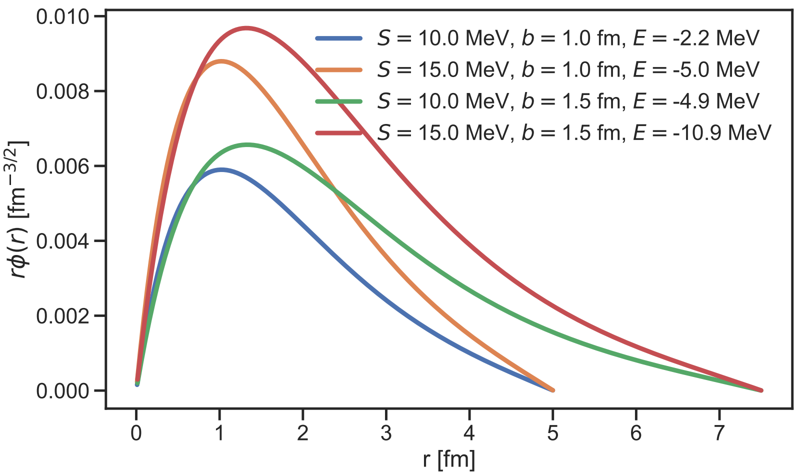

Figure 3.6: Radial wave functions for different parameters as shown in the legend.

The shapes of the radial wave functions are similar to the Gaussian case, but the energies do not match due to the r^2/b^2 dependency in the Gaussian case. One could argue for a Yukawa-like form factor but with a gaussian exponential, $\exp\left(r^2/b^2\right)/r$, and the energies are the same within a few MeV, but this defeats the purpose of a Yukawa form. An exponential form factor would make the radial wave function too long to describe the nuclear range since we are constrained to about 15 fm.

3.4.2 Relativistic Expansion

As described in section 3.1, we are using the Schrödinger equation, which hints at a non-relativistic limit of the pion-nucleon system. We also know the pion is virtual, which means under a potential barrier. An avant-garde idea is to do relativistic expansion of the kinetic term, which depends on the relative coordinate $\mathbf{r}$.

The pion is virtual, which makes the velocity of the particle hard to estimate–nonetheless, we can do an expansion of the kinetic operator and see how this affects the model. To account for relativistic effects, we can replace the kinetic term, $K_\mathbf{r}$ in (3.17)

$$K_\mathbf{r} \longrightarrow K_{\mathbf{r},\mathrm{rel}} = \sqrt{p^2c^2 + \mu_{N\pi}^2 c^4} = \mu_{N\pi}c^2\left(\sqrt{1 + \frac{p^2}{\mu_{N\pi}^2 c^2}} - 1\right), \tag{3.32}$$

where $\mu_{N\pi}$ is the reduced mass of the nucleon-pion system. This leads to a new system of equations, and these solutions can be compared to the non-relativistic limit to deduce which relativistic regime dominates the system. Starting from (3.19)

$$f(r)(\boldsymbol{\tau}\cdot\boldsymbol{\pi})(\boldsymbol{\sigma}\cdot\mathbf{r})\psi_p + \mu_{N\pi}c^2\left(\sqrt{1+\frac{p^2}{\mu_{N\pi}^2c^2}}-1\right)\psi_{N\pi} = (E-m_\pi c^2)\psi_{N\pi}, \tag{3.33}$$

This equation turns out to be divergent, and we must therefore resort to an approximation. The kinetic energy is expanded

$$K_{\mathbf{r},\mathrm{rel}} = \mu_{N\pi}c^2\sqrt{1+\frac{p^2}{\mu_{N\pi}^2}} - \mu_{N\pi}c^2 \approx \frac{p^2}{2\mu_{N\pi}} - \frac{p^4}{8\mu_{N\pi}^3c^2} \tag{3.34}$$

This means we get an extra term in (3.22), yielding

$$(\boldsymbol{\tau}\cdot\boldsymbol{\pi})(\boldsymbol{\sigma}\cdot\mathbf{r})f(r)\frac{p\uparrow}{\sqrt{V}} + \left(\frac{p^2}{2\mu_{N\pi}} - \frac{p^4}{8\mu_{N\pi}^3c^2}\right)(\boldsymbol{\tau}\cdot\boldsymbol{\pi})(\boldsymbol{\sigma}\cdot\mathbf{r})\frac{p\uparrow}{\sqrt{V}}\phi(r) = (E-m_\pi c^2)(\boldsymbol{\tau}\cdot\boldsymbol{\pi})(\boldsymbol{\sigma}\cdot\mathbf{r})\phi(r)\frac{p\uparrow}{\sqrt{V}}, \tag{3.35}$$

Using the vector operators yields the following expression[5]

$$f(r) - \frac{\hbar^2}{2\mu_{N\pi}}\left(\phi^{(2)}(r)+\frac{4}{r}\phi^{(1)}(r)\right) - \frac{\hbar^4}{8\mu_{N\pi}^3c^3}\left(\phi^{(4)}(r)+\frac{6}{r}\phi^{(3)}(r)\right) = (E-m_\pi c^2)\phi(r), \tag{3.36}$$

5. $$\nabla^4(\mathbf{r}\phi(r)) = \mathbf{r}\left(\phi^{(4)}+\frac{6}{r}\phi^{(3)}\right)$$

where the exponent, (n), is the order of the differentiation. This leads to a system of equations given by

$$\left.\begin{array}{l} 12\pi\int_0^\infty \mathrm{d}r\, f(r)\phi(r)r^4 = E \\ f(r) - \frac{\hbar^2}{2\mu_{N\pi}}\left(\phi^{(2)}(r)+\frac{4}{r}\phi^{(1)}(r)\right) - \frac{\hbar^4}{8\mu_{N\pi}^3c^3}\left(\phi^{(4)}(r)+\frac{6}{r}\phi^{(3)}(r)\right) = (E-m_\pi c^2)\phi(r) \end{array}\right\} \tag{3.37}$$

This system is a fourth-order differential equation coupled to an integrodifferential equation and is solved using the boundary value problem technique. The boundary conditions can be found using the same considerations as in the previous section. For $r\longrightarrow\infty$ the dominating terms are

$$\phi^{(4)}(r) = \frac{-8\mu_{N\pi}c^2}{\hbar^4}(E-m_\pi c^2)\phi(r) - \frac{4\mu_{N\pi}^2c^2}{\hbar^2}\phi(r)^{(2)} \tag{3.38}$$

The solutions are shown in figure 3.7 where only $\phi(r)$ and $\phi(r)^{(1)}$ are included using the Gaussian form factor

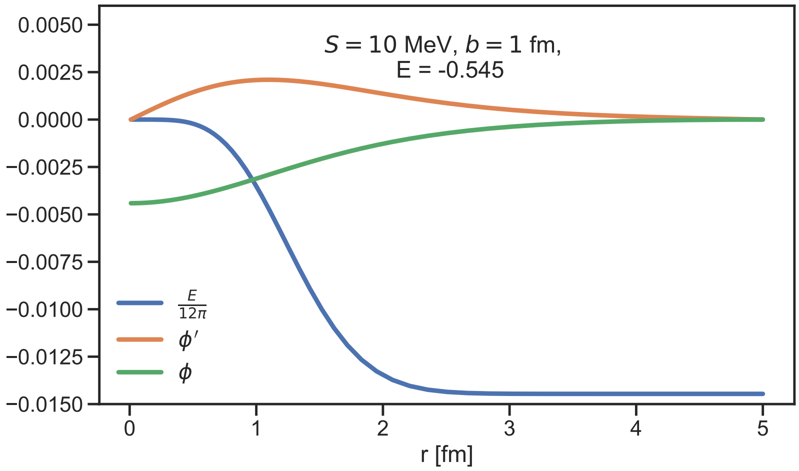

Figure 3.7: Boundary value problem solutions for the relativistic expansion using the Gaussian form factor. The energy convergence is scaled.

We gain information about the system both from the wave function and the energy, and we consider these two components of figure 3.7 separately. The radial wave function of the system can be seen in figure 3.8

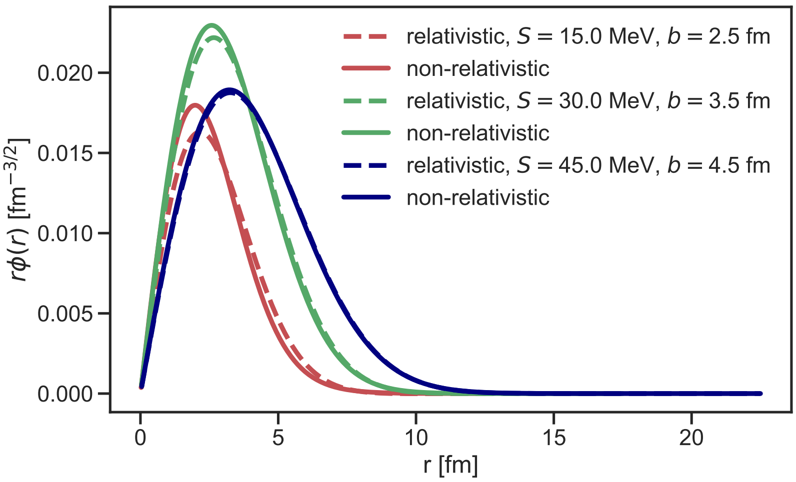

Figure 3.8: Relativistic (dashed) and non-relativistic radial wave functions for three different parameters. The matching colours have the same parameters

The radial wave functions are similar, with the lowest strength parameter S and range parameter b having the largest difference. This can be explained by considering equation (3.37). The form factor $f(r)$ depends explicitly on the ratio between these two parameters in the same way in the relativistic limit as in the non-relativistic limit. However, the form factor can change by orders of magnitude by varying the two parameters, and this will only affect the solution $\phi(r)$ regarding when the form factor vanishes and the $r \to \infty$ limit applies. This also means we should expect the energy ratio between the non-relativistic equation (3.24) and equation (3.37) to approach 1 as the range parameter b increases since this decreases the impact of the form factor. This is shown in figure 3.9, where the energy ratio is given by

$$E_R = \frac{E_{\text{relativistic}}}{E_{\text{non-relativistic}}}. \tag{3.39}$$

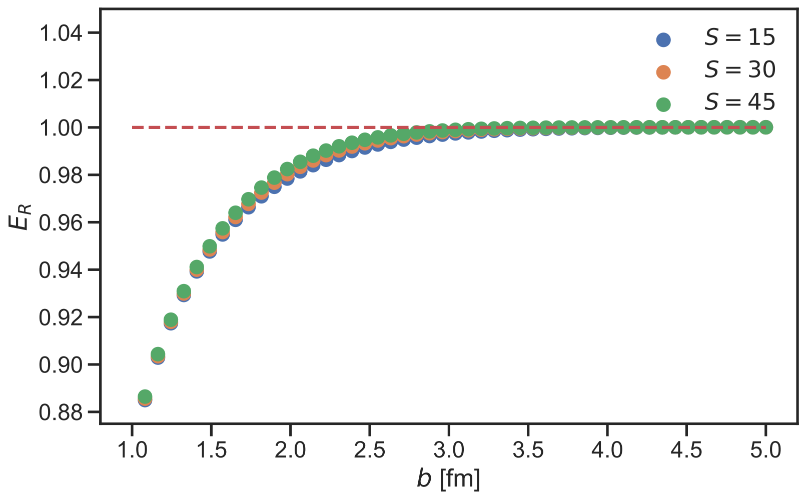

Figure 3.9: The energy ratio $E_{\text{rel}}/E_{\text{nonrel}}$ shown as a function of the range parameter b for a Gaussian form factor given by equation (3.6)

We can apply the same logic to the system of equations with a Yukawa-like form factor as in equation (3.31), and we expect the same convergence. This is shown on figure 3.10

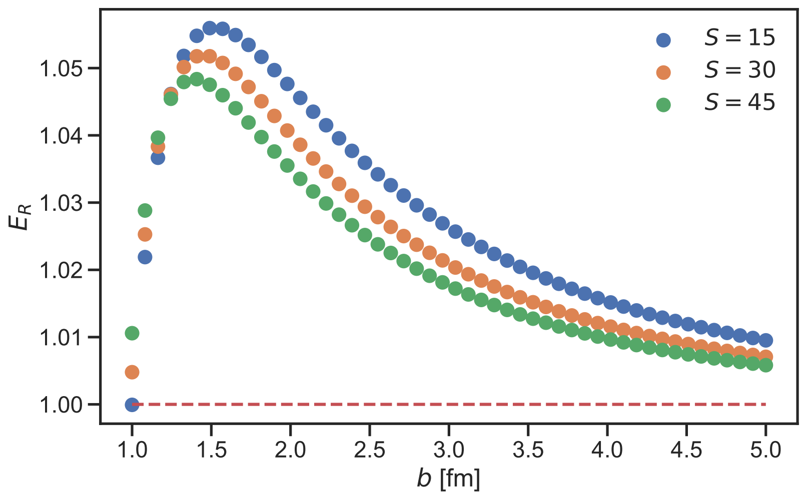

Figure 3.10: The energy ratio $E_{\text{rel}}/E_{\text{nonrel}}$ shown as a function of the range parameter b for a Yukawa-like form factor given by equation (3.31)

The pion is virtual and hence in a classically forbidden region, but we can still estimate which relativistic regime dominates the system. Both in terms of the radial wave function and in terms of the energy ratio, relativistic effects are negligible. This result holds for different form factors since they must all decrease a function of r.

Considering figure 3.9, we see the maximum discrepancy between the relativistic and the non-relativistic energy is about 10 per cent and decreases rapidly. This means relativistic effects vanish as we increase the range parameter b. A physical explanation of this could be that as we increase the spatial dimension, a virtual pion with the same kinetic energy would have a lower velocity and hence less relativistic. This analysis is supported if the same behaviour is not present when we hold b fixed an increase S since. This is shown in figure 3.11 for the Gaussian form factor

Figure 3.11: The energy ratio $E_{\text{rel}}/E_{\text{nonrel}}$ shown as a function of the strength parameter b for a Yukawa-like form factor given by equation (3.31)

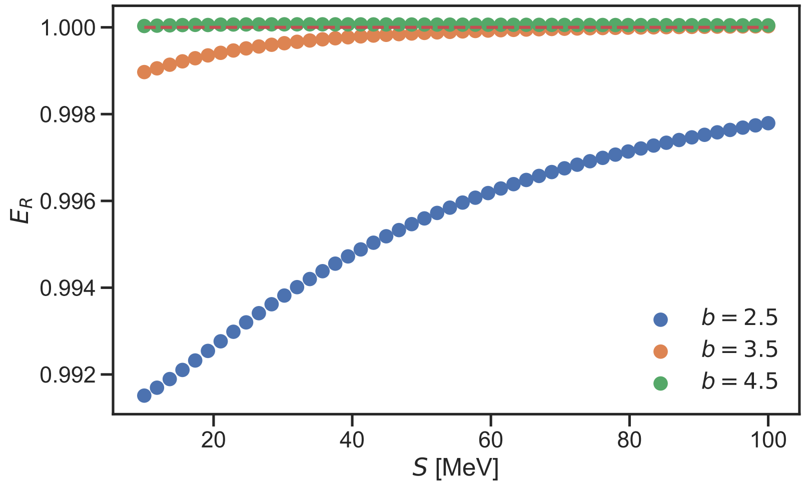

A similar plot for the Yukawa-like form factor

Figure 3.12: The energy ratio $E_{\text{rel}}/E_{\text{nonrel}}$ shown as a function of the strength parameter S for a Yukawa-like form factor given by equation (3.31)

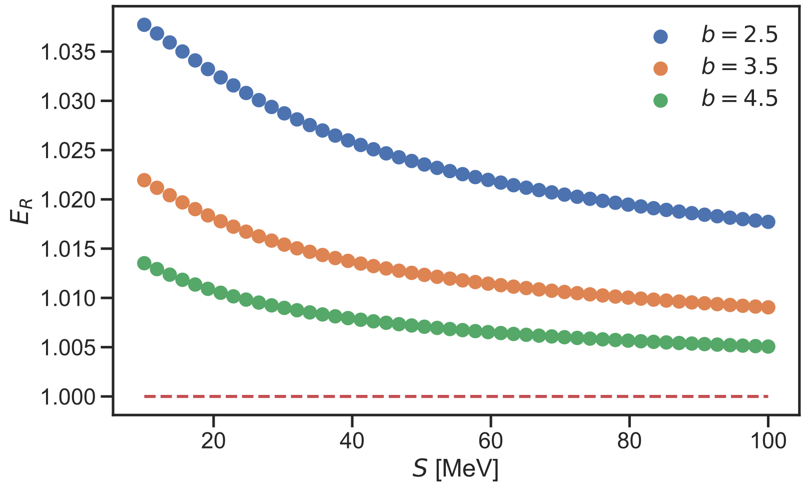

3.4.3 Nuclear Effective Field Theory Operator

The construction of the most general chiral Lagrangian is based on the theory of the non-linear realisation of symmetry [8]. The baryon-number-conserving chiral Lagrangian can be split into pieces with even numbers of fermion fields where in this section, we will focus on

$$\mathcal{L} = N^\dagger \left(i\mathcal{D}_0 + \frac{\mathcal{D}^2}{2m_N} \right) N + \frac{g_A}{2f_\pi} N^\dagger \boldsymbol{\tau} N \cdot \mathbf{D}\boldsymbol{\pi}, \tag{3.40}$$

where the second term is very similar to the creation operator W from equation (3.2)–only the $\mathbf{r}$ is replaced by $\nabla_{\mathbf{r}}$. The general operator is constructed in such a way that parity, isospin and spin are conserved, and there is some freedom in the choice of the distance operator. In this section, we explore the differences by constructing the nuclear model with explicit mesons with the operator as defined in chiral effective field theory. We assume the following form of the wave function of the proton and the system consisting of a nucleon and a single pion

$$\psi_p = p \uparrow \frac{1}{\sqrt{V}}, \quad \psi_{N\pi} = (\boldsymbol{\tau} \cdot \boldsymbol{\pi})(\boldsymbol{\sigma} \cdot \frac{\partial}{\partial \mathbf{r}}) p \uparrow \frac{1}{\sqrt{V}} \phi(r), \tag{3.41}$$

where $\boldsymbol{\tau}$ and $\boldsymbol{\sigma}$ are vectors consisting of Pauli matrices acting on isospin and spin space on the nucleon, respectively. $\boldsymbol{\pi}$ is the isovector of pions. We now construct an operator to create and annihilate a pion

$$W = (\boldsymbol{\tau} \cdot \boldsymbol{\pi})(\boldsymbol{\sigma} \cdot \frac{\partial}{\partial \mathbf{r}})f(r) \tag{3.42}$$

$$W^\dagger = \int_V \mathrm{d}^3 r\, (\boldsymbol{\tau} \cdot \boldsymbol{\pi})^\dagger (\boldsymbol{\sigma} \cdot \frac{\partial}{\partial \mathbf{r}})^\dagger f(r), \tag{3.43}$$

where $f(r)$ is a form factor. The annihilation operator must contain the integral to remove the coordinate of the pion. This leads to the following Schrödinger equation

$$\begin{bmatrix} K_{\mathbf{R}} & W^\dagger \\ W & K_{\mathbf{R}} + K_{\mathbf{r}} + m_\pi c^2 \end{bmatrix} \begin{bmatrix} \psi_p \\ \psi_{N\pi} \end{bmatrix} = E \begin{bmatrix} \psi_p \\ \psi_{N\pi} \end{bmatrix}, \tag{3.44}$$

which is expanded

$$12\pi \int_0^\infty \mathrm{d}r\, \frac{\partial^2}{\partial r^2} r^2 f(r)\phi(r) = E \tag{3.45}$$

$$\frac{\partial}{\partial r} f(r) - \frac{2\hbar^2}{\mu_{N\pi}} \frac{\partial^3}{\partial r^3}\phi(r) = (E - m_\pi c^2)\frac{\partial}{\partial r}\phi(r). \tag{3.46}$$

Assume the form factor is on the following form

$$f(r) = \frac{S}{b} \mathrm{e}^{-r^2/b^2} \tag{3.47}$$

which yields

$$\frac{\partial}{\partial r} f(r) = \frac{-2r}{b^2} f(r), \qquad \frac{\partial^2}{\partial r^2} = -\frac{2(b^2 - 2r^2 2)}{b^4} f(r). \tag{3.48}$$

The terms inside the integral in equation (3.45)

$$\frac{\partial^2}{\partial r^2}(r^2 f(r)\phi(r)) = 2r f(r)\phi(r) + 2r f'(r)\phi(r) + r^2 f(r)\phi'(r) \tag{3.49}$$

$$+ 2r f'(r)\phi(r) + r^2 f''^{(r)}\phi(r) + r^2 f'(r)\phi'(r) \tag{3.50}$$

$$+ 2r f(r)\phi(r) + r^2 f'(r)\phi'(r) + r^2 f(r)\phi''(r) \tag{3.51}$$

$$\equiv Y(r) \tag{3.52}$$

Considering the limits of (3.46) which for large r is

$$\phi'''(r) = \frac{-\mu_{N\pi}}{2\hbar^2}(E - m_\pi c^2)\phi'(r) \tag{3.53}$$

The solution is shown on 3.13

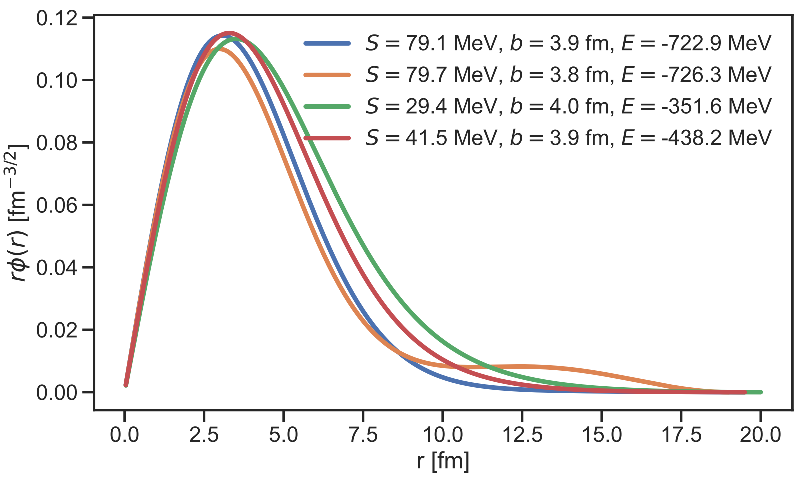

Figure 3.13: The radial wave function using the operator form from an effective field theory.

The parameters S and b in the radial wave functions are not the same as in figure 3.5 and figure 3.6 but should better represent actual parameter values when performing the fit to the total cross-section data. This is done to better highlight this model's validity and some of its disadvantages. The energies are within the same order of magnitude as when using the model described in section 3.3. There is a difference in energy, and this model could be investigated further – however, this model using the nuclear effective field theory's operator is a lot more numerically intensive. Due to the derivative in equation (3.41), (3.42) and (3.43), we got many more terms as seen in (3.52), which all have to be integrated numerically. Perhaps another numerical method is better suited for this operator type.

Chapter 4

Pion Photoproduction

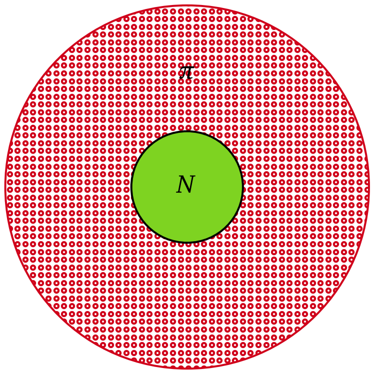

Figure 4.1: Illustration of the dressed nucleon. In the centre (green) is a nucleon, and surrounding it is a cloud of virtual pions (red gradient).

We now consider the case of pion photoproduction. In the model mentioned in section 3.1 the nucleon is in a superposition of states with an arbitrary number of pions. However, we constrain the model to the one-pion approximation. This is illustrated in figure 4.1

There are four pion photoproduction processes on nucleons, and these are given by

$$p\gamma \longrightarrow p\pi^0 \tag{4.1}$$
$$p\gamma \longrightarrow n\pi^+ \tag{4.2}$$
$$n\gamma \longrightarrow n\pi^0 \tag{4.3}$$
$$n\gamma \longrightarrow p\pi^- . \tag{4.4}$$

Within the framework of this model, we would expect these processes by applying the equation (3.4) to the isospin state of the given nucleon, i.e.

$$(\boldsymbol{\tau} \cdot \boldsymbol{\pi})p = p\pi^0 + \sqrt{2}n\pi^+, \tag{4.5}$$

and similarly for the isospin state of the neutron. As mentioned in section 3.3, the pion is trapped behind a potential barrier of height 140 MeV and cannot leave unless an incoming photon of sufficient energy hits the pion-nucleon system and photodisintegrates the virtual pion and creates a physical pion in the process. This means pion photoproduction comes naturally as a photodisintegration process. Consider some initial bound state represented by the following two-component wave function

$$|\Phi_i\rangle = \begin{bmatrix} \phi_p \\ \phi_{N\pi} \end{bmatrix}, \tag{4.6}$$

where ϕ represents a bound state. The final state consists of the same superposition but in an unbound system represented by ψ, i.e.

$$\left|\Psi_f\right\rangle = \begin{bmatrix} \psi_p \\ \psi_{N\pi} \end{bmatrix}. \tag{4.7}$$

The two-component wave function photodisintegration is similar to the photodisintegration process of the deuteron[1]. We can apply a similar approach and get an expression for the total cross section as a function of energy and the strength parameter S, and the range parameter b. The general idea is to fit the parameters to experimental data such that we get a set of parameters within which the model can describe the total cross-section near the threshold. We constrain the model to only apply near the threshold since we expect more pions are needed to describe the total cross section at higher energies adequately. The advantages of this

1. This is covered in appendix A

model are twofold: the reduced number of parameters allows us to fit the model to experimental data efficiently, and the model's generality will enable us to apply these parameters to a different process accounting only for the difference in mass and isospin coefficient. Also, in the case of the pion photoproduction process (4.1) is very well investigated while (4.2) and (4.3) have limited data and (4.4) have none near the threshold. Our first approach is to apply a dipole approximation since we are considering the photoproduction processes near the threshold.

4.1 Dipole Approximation

We want to calculate the total cross-section of pion photoproduction off nucleons. In this section, we focus on the process involving charged pions off protons given by equation (4.2). The general idea is to use Fermi's golden rule, and this involves a matrix element expressed in terms of equation (4.6) and equation (4.7)

$$\left\langle \Psi_f \middle| \mathbf{d} \middle| \Phi_i \right\rangle, \tag{4.8}$$

where a dipole operator $\mathbf{d}$. Equation (4.8) just means we use the dipole operator on some initial bound state, and the final state consists of an unbound system. We start from the general expression of the multi-component wave function and impose a normalisation to both the initial and final state. Starting from (4.6)

$$\Phi = \mathcal{N}\begin{bmatrix} p\uparrow \\ (\boldsymbol{\tau}\cdot\boldsymbol{\pi})(\boldsymbol{\sigma}\cdot\mathbf{r})p\uparrow\phi(r) \end{bmatrix}, \tag{4.9}$$

where $\uparrow$ represents the spin state, $\phi(r)$ is the wave function from figure 3.4 and $\mathcal{N}$ is the normalisation constant. This leads to

$$\begin{aligned} \langle\Phi|\Phi\rangle &= |\mathcal{N}|^2\left(\left\langle\phi_p\middle|\phi_p\right\rangle + \left\langle\phi_{N\pi}\middle|\phi_{N\pi}\right\rangle\right) && (4.10)\\ &= |\mathcal{N}|^2\left(V + 3V\int \mathrm{d}^3r\, r^2\phi(r)^2\right) && (4.11)\\ &\overset{!}{=} 1. && (4.12) \end{aligned}$$

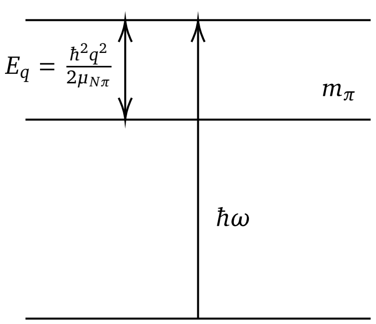

Figure 4.2: Energy diagram of the system. Here $\mu_{N\pi}$ is the reduced mass of the pion-nucleon system. The lowest vertical line corresponds to the threshold.

This leads to the following normalisation constant

$$\mathcal{N} = \frac{1}{\sqrt{V}}\frac{1}{\sqrt{1+\epsilon}}, \tag{4.13}$$

where V is the volume and ϵ is the integral in (4.11)–numerically, this is close to unity. This expression is the properly normalised initial state.

The final state consists of the unbound system represented by ψ. We know the final state consists of a plane wave with wave number $\mathbf{q}$ propagating along the z-axis. The wave number $\mathbf{q}$ is written in terms of the pion-nucleon momentum, and the magnitude of this is given by

$$\frac{\hbar^2 q^2}{2\mu_{N\pi}} = \hbar\omega - m_\pi c^2, \tag{4.14}$$

which is also illustrated in figure 4.2. The plane wave can be represented by

$$\mathrm{e}^{iqz} = \mathrm{e}^{i\mathbf{q}\cdot\mathbf{r}}, \tag{4.15}$$

where θ is the angle between $\mathbf{q}$ and $\mathbf{r}$ illustrated on **??**. Using orthogonality and the addition theorem for the spherical harmonics, we can decompose the plane wave into a Bessel function and spherical harmonics[2]. This yields

2. See equation (B.9)

$$\frac{1}{\sqrt{V}}\mathrm{e}^{-i\mathbf{q}\cdot\mathbf{r}} = \frac{1}{\sqrt{V}}\sum_{\ell,m} 4\pi i^{\ell} Y_{\ell}^{*m}(\mathbf{q})Y_{\ell}^{m}(\mathbf{r})j_{\ell}(qr) \tag{4.16}$$

$$= \frac{1}{\sqrt{V}}\sum_{\ell} 4\pi i^{\ell} j_{\ell}(qr)\left(\frac{2\ell+1}{4\pi}\right)P_{\ell}(\cos\theta), \tag{4.17}$$

and P_ℓ is the Legendre polynomial of degree ℓ. Since we are considering the energies close to the threshold, we expect mainly the S-wave to contribute and ignore higher orders[3]. We should empathise that this is an approximation, and a priori, we do not know to what degree this holds. In terms of the expansion (4.16), this greatly simplified the expression

3. Threshold behaviour when $\lambda \simeq 1/q \gg R$ where R is the range higher orders of ℓ are generally not important [12].

$$\frac{1}{\sqrt{V}}\mathrm{e}^{i\mathbf{q}\cdot\mathbf{r}} \overset{\ell=0}{=} \frac{1}{\sqrt{V}}j_0(qr). \tag{4.18}$$

As equation (4.18) shows, we are left with a spherical Bessel function in the final state where the volume is kept to stress that the total cross section must be independent of the volume. To calculate the matrix element, we return to equation (2.1) and consider the electric field given by

$$\mathcal{E} = -\frac{1}{c}\frac{\partial \mathbf{A}}{\partial t}. \tag{4.19}$$

The interaction operator in the dipole approximation is given by

$$H_{\text{dipole}} = -\mathcal{E}(\mathbf{r}=0)\cdot\mathbf{d}, \tag{4.20}$$

where $\mathbf{d}$ is the dipole moment of the pion-nucleon system given by

$$\mathbf{d} = e\frac{\mu_{N\pi}}{m_\pi}\mathbf{r}. \tag{4.21}$$

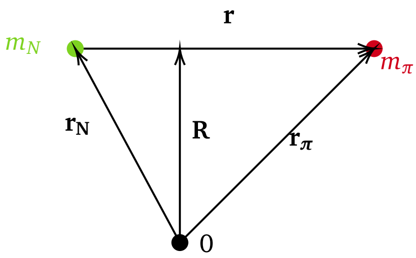

Figure 4.3: Relative coordinates of the pion-nucleon system.

The general setup for the system is shown in figure 4.3, where the nucleon, in this case, is a proton. Considering a general pion photoproduction process on the form

$$N+\gamma \rightarrow N+\pi \tag{4.22}$$

allows us to calculate the electromagnetic part of the matrix element. The initial state consists of the dressed nucleon and a photon $a^\dagger_{\mathbf{k},\lambda}|0\rangle$, where $|0\rangle$ is the electromagnetic vacuum state. The final state consists of a nucleon, a pion and the electromagnetic vacuum. This means the transition in the dipole approximation is given by

$$\langle 0|\mathcal{E}a^\dagger_{\mathbf{k},\lambda}|0\rangle = \sqrt{\frac{2\pi\hbar}{\omega_k V}}\, i\omega_k \mathbf{e}_{\mathbf{k},\lambda}\mathrm{e}^{-i\omega_k t}, \tag{4.23}$$

which combined with Fermi's golden rule

$$\mathrm{d}\omega = \frac{2\pi}{\hbar}|\mathcal{M}|^2\,\mathrm{d}\rho, \tag{4.24}$$

describes the probability per unit of time of making a transition. Equation (4.23) is the most general expression we can make, and in this section, consider the S-wave channel for the process (4.2). Calculations for (4.1), (4.3) and (4.4) are very similar. Calculating the matrix element

$$\mathcal{M} = \langle \frac{j_0(qr)}{\sqrt{V}} n\pi^+(\uparrow\downarrow)|H_{\text{dipole}}|\psi_{N\pi}\mathcal{N}\rangle \tag{4.25}$$

Plugging in equation (4.25) and (4.9)

$$\mathcal{M} = -i\omega_k\sqrt{\frac{2\pi\hbar}{V\omega_{\mathbf{k}}}}\mathbf{e}_{\mathbf{k},\lambda}\,\langle\frac{1}{\sqrt{V}}j_0(qr)n\pi^+(\uparrow\downarrow)|\mathbf{d}|(\boldsymbol{\tau}\cdot\boldsymbol{\pi})(\boldsymbol{\sigma}\cdot\mathbf{r})p\uparrow\phi(r)\mathcal{N}\rangle \tag{4.26}$$

where the two arrows represent the two spin states of the neutron and the proton. The different spin states of the neutron in the final state yield two contributions to the total matrix element given by

$$\mathcal{M}^{\uparrow} = \frac{-i\mathcal{N}\sqrt{2}\omega_k\mathbf{e}_{\mathbf{k},\lambda}}{V}\sqrt{\frac{2\pi\hbar}{V\omega_{\mathbf{k}}}}\sqrt{\frac{4\pi}{3}}\,\langle j_0(qr)|d_0 rY_1^0|\phi(r)\rangle \tag{4.27}$$

$$\mathcal{M}^{\downarrow} = \frac{-i\mathcal{N}2\omega_k\mathbf{e}_{\mathbf{k},\lambda}}{V}\sqrt{\frac{2\pi\hbar}{V\omega_{\mathbf{k}}}}\sqrt{\frac{4\pi}{3}}\,\langle j_0(qr)|d_0 rY_1^1|\phi(r)\rangle\,, \tag{4.28}$$

$$\tag{4.29}$$

where the spin-down state picks up a factor $\sqrt{2}$ from equation (3.5). Now we calculate the remaining matrix elements,

$$\left\langle j_0(qr)\middle|d_0r_0\middle|\phi(r)\right\rangle = \frac{\mu_{N\pi}}{m_\pi}e\left\langle j_0(qr)\middle|r_0r_0\middle|\phi(r)\right\rangle \tag{4.30}$$

$$= \frac{\mu_{N\pi}}{m_\pi}e\frac{4\pi}{3}\left\langle j_0\middle|r^2\middle|\phi(r)\right\rangle \tag{4.31}$$

$$= \frac{4\pi\mu_{N\pi}e}{3m_\pi}\underbrace{\int_0^\infty \mathrm{d}r\; j_0(qr)r^4\phi(r)}_{Q(r)}, \tag{4.32}$$

where the dipole operator (4.21) has been inserted and the angular integrals calculated. We have also introduced an integral, which contains the wave function $\phi(r)$. Similarly, for the next matrix element,

$$\left\langle j_0(qr)\middle|d_-r_+\middle|\phi(r)\right\rangle = \frac{\mu}{m_\pi}e\left\langle j_0(qr)\middle|r_-r_+\middle|\phi(r)\right\rangle \tag{4.33}$$

$$= \frac{4\pi\mu e}{3m_\pi}\left\langle j_0(qr)\middle|r^2Y_1^{-1}Y_1^1\middle|\phi(r)\right\rangle \tag{4.34}$$

$$= \frac{4\pi\mu e}{3m_\pi}Q(r). \tag{4.35}$$

It turns out these two matrix elements are equal. Taking the norm-square of (4.32)

$$\left|\mathcal{M}^{\uparrow}\right|^2 = \left(\frac{4\pi\mu e}{3m_\pi}\right)^2\frac{2\mathcal{N}^2\omega_k(2\pi\hbar)}{V^2}(\mathbf{e}_{\mathbf{k},\lambda})^0(\mathbf{e}^*_{\mathbf{k},\lambda})^0Q(r)^2 \tag{4.36}$$

Similarly, for the equation (4.35)

$$\left|\mathcal{M}^{\downarrow}\right|^2 = \left(\frac{4\pi\mu e}{3m_\pi}\right)^2\frac{4\mathcal{N}\omega_{\mathbf{k}}(2\pi\hbar)}{V^2}(\mathbf{e}_{\mathbf{k},\lambda})^+(\mathbf{e}^*_{\mathbf{k},\lambda})^+Q(r)^2. \tag{4.37}$$

Calculating the total matrix element using a polarization theorem[4]

$$|\mathcal{M}|^2 = \left|\mathcal{M}^{\uparrow}\right|^2 + \left|\mathcal{M}^{\downarrow}\right|^2 \tag{4.38}$$

$$= \frac{2\pi\hbar\omega_k\mathcal{N}^2e^2}{V^2}\left(\frac{4\pi\mu}{3m_\pi}\right)^2Q(r)^2, \tag{4.39}$$

which is the final expression for the matrix element. According to Fermi's golden rule (4.24) and the non-relativistic density of states (2.19), we

4. $(\mathbf{e}^*_{\mathbf{k},\lambda}\cdot\mathbf{e}_{\mathbf{k},\lambda}) = \delta_{\lambda,\lambda'}$ and $\mathbf{e}_{\mathbf{k},\mp} = \pm\frac{1}{\sqrt{2}}(\mathbf{e}_{\mathbf{k},1}\pm i\mathbf{e}_{\mathbf{k},2})$. This leads to $(\mathbf{e}^{0*}_{\mathbf{k},\lambda}\cdot\mathbf{e}^0_{\mathbf{k},\lambda'})+(\mathbf{e}^{0+}_{\mathbf{k},\lambda}\cdot\mathbf{e}^+_{\mathbf{k},\lambda'}) = \delta_{\lambda,\lambda'}+\frac{1}{2}\delta_{\lambda,\lambda'}$

get the transition probability. To go from the transition probability to the differential cross-section, we need to consider the flux density of the photons. This means a factor V/c, where V is the volume, and c is the speed of light. This leads to the final expressions for the differential cross-section.

$$\frac{d\sigma^+}{d\Omega_q} = \frac{16\pi}{9}\mathcal{N}^2\alpha\frac{kq\mu_{N\pi}^3}{m_\pi^2\hbar c}Q(r)^2, \tag{4.40}$$

where the + is used to indicate that this is the expression for positively charged pions in the final state. Since there is no explicit angular dependency, the total cross-section is given by

$$\sigma_{\text{dipole}}^+ = \oint_{4\pi}\frac{d\sigma}{d\Omega_q}d\Omega_q \tag{4.41}$$

$$= \frac{64\pi^2}{9}\mathcal{N}^2\alpha\frac{kq\mu_{N\pi}^3}{m_\pi^2\hbar c}\left(\int_0^\infty dr\, j_0(qr)r^4\phi(r)\right)^2. \tag{4.42}$$

This is the final expression for the total cross-section of the photoproduction of charged pions using the dipole approximation. We now perform a fit to experimental data for the parameters S and b and enter in the wave function $\phi(r)$. Here two considerations are needed. Both the dipole approximation and the one-pion approximation limit the validity of the cross-section to near the threshold. Quantitatively the dipole approximation holds when

$$\lambda \simeq 1/q \gg R, \tag{4.43}$$

where R is the range of the system. In nuclei, the condition (4.43) is equivalent to

$$\hbar\omega \ll 165A^{1/3}, \tag{4.44}$$

which limits our dipole approximations area of validity to approximately 15 MeV from the threshold. Equation (4.42) is fitted to experimental data for the parameters S and b and is shown in figure 4.4

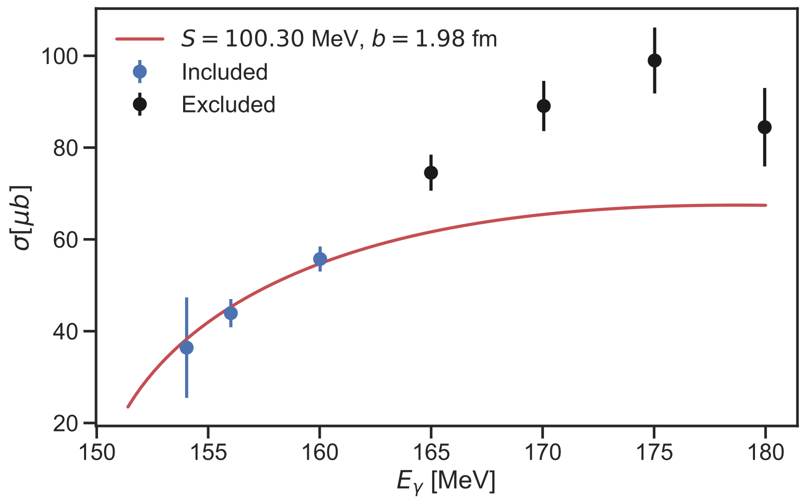

Figure 4.4: The total cross-section of the photoproduction process $\gamma p \longrightarrow \pi^+ n$ fitted to experimental data. The fit parameters are shown in the figure. The blue data points are included in the fit, and the black data points are excluded since these violate both the dipole and the one pion approximation.

Note here that we have used two approximations that limit (4.42) to energies very close to the threshold. We need a more general expression for the cross-section and more data points to test the model's validity further. This means we have to consider the exact matrix element for the transition and consider the photoproduction of neutral pions off protons since this is the most experimentally investigated photoproduction process.

4.2 Exact Matrix Element

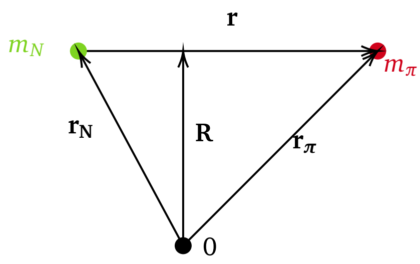

Figure 4.5: Sketch of the system. Here $\mathbf{r}_N$ is the coordinate of the proton and $\mathbf{r}_\pi$ is the coordinate of the pion. The relative coordinate is given by $\mathbf{r} = \mathbf{r}_\pi - \mathbf{r}_p$ and the coordinate of the center-of-mass is $\mathbf{R} = (m_p \mathbf{r}_p + m_\pi \mathbf{r}_\pi)/(m_p + m_\pi)$. The total mass is denoted $M_{p\pi} = m_p + m_\pi$.

In section 4.1, we looked at how to use the model described in section 3.1 to get an expression for the cross-section, which was compared to experimental data. More specifically, we used the dipole approximation, which introduces a trade-off between the difficulty of the calculations and the regime in which our solution is valid. We expect the dipole approximation to hold for energies just above the threshold. To both validate and generalise this result, we now make a different approach and calculate the exact cross-section and also consider recoil effects and apply this approach to the four photoproduction processes using the density of states in the non-relativistic and relativistic limits. Strictly speaking, recoil effects should also be considered in section 4.1 since the mass ratio between the nucleon and the pion cannot be assumed to yield a stationary nucleon after the pion photoproduction process.

To calculate the exact matrix elements, we consider a non-relativistic system of particles interacting with the electromagnetic field as described in section 2.1. We have to keep in mind that equation (2.7) describes how a particle with charge interacts with the electromagnetic field. This means if we consider a process where the initial state is a dressed neutron, the pion must be responsible for the interaction with the electromagnetic field. We will consider the four pion photoproduction processes separately even though the calculations are very similar. In general, we will consider a system illustrated in figure 4.5, which shows the pion-nucleon system, and in terms of the Jacobi coordinates, we get the following expressions for the coordinates of the particles

$$\mathbf{r}_N = \mathbf{R} - \frac{m_\pi}{M_{N\pi}} \mathbf{r} \tag{4.45}$$

$$\mathbf{r}_\pi = \mathbf{R} + \frac{m_N}{M_{N\pi}} \mathbf{r}, \tag{4.46}$$

where $\mathbf{R}$ is the coordinate of the center of mass of the pion-nucleon system given by

$$\mathbf{R} = \frac{m_N \mathbf{r}_N + m_\pi \mathbf{r}_\pi}{M_{N\pi}}, \quad M_{N\pi} = m_N + m_\pi. \tag{4.47}$$

The relative coordinate is given by

$$\mathbf{r} = \mathbf{r}_\pi - \mathbf{r}_N. \tag{4.48}$$

The general approach is the same as in section 3.3, where we want to use Fermi's golden rule to calculate the total cross-section. In this section, we also consider the impact of changing the density of states to the relativistic case. Furthermore, we estimate the relative weight of the pion component in the wave function of the dressed nucleon. We do this by introducing the following

$$C(\psi_{N\pi}) = \int_V \mathrm{d}^3 R \int_V \mathrm{d}^3 r \left|\psi_{N\pi}\right|^2, \tag{4.49}$$

where per construction of the model, this is dimensionless. We also introduce a parameter to estimate the virtual pions' contribution to the mass of the dressed nucleon. This will be denoted Π and corresponds to the energy found by solving (3.24).

4.2.1 Neutral Pion Photoproduction off Protons

We are considering the process

$$p\gamma \longrightarrow \pi^0 p, \tag{4.50}$$

where the proton interacts with the electromagnetic field. From equation (2.7) we get

$$H^{(1)} = -\frac{e}{m_p c}\mathbf{A}(\mathbf{r}_p, t)\cdot\mathbf{p}_p, \tag{4.51}$$

where $\mathbf{p}_p$ is the momentum operator of the proton. Equation (4.51) can be rewritten in terms of the relative coordinates

$$H^{(1)} = -\frac{e}{m_p c}\mathbf{A}\left(\mathbf{R} - \frac{m_\pi}{M_{p\pi}}\mathbf{r}, \mathbf{t}\right)\cdot\left(\frac{m_p}{M_{p\pi}}\mathbf{P} - \mathbf{p}\right) \tag{4.52}$$

In equation (4.50), the initial state consists of a dressed proton and a plane wave photon in the state $a^\dagger_{\mathbf{k},\lambda}\left|0\right\rangle$ where $\mathbf{k}$ is the wave number and λ the polarisation index. The final state consists of a proton and a π^0 in a relative plane wave motion. The electromagnetic part of the matrix element is

$$-\frac{e}{m_p c}\left\langle 0|\mathbf{A}(\mathbf{r}_p, t)a^\dagger_{\mathbf{k},\lambda}|0\right\rangle = -\frac{e}{m_p c}\sqrt{\frac{2\pi\hbar}{\omega_k V}}\mathbf{e}_{\mathbf{k},\lambda}\mathrm{e}^{i\mathbf{k}\cdot\mathbf{r}_p - i\omega_k t} \tag{4.53}$$

$$= -\frac{e}{m_p c}\sqrt{\frac{2\pi\hbar}{\omega_k V}}\mathbf{e}_{\mathbf{k},\lambda}\mathrm{e}^{i\mathbf{k}(\mathbf{R} - \frac{m_\pi}{M_{p\pi}}\mathbf{r}) - i\omega_k t}. \tag{4.54}$$

We now return to equation 4.52 where we set $\mathbf{P} = 0$, which corresponds to moving to the lab frame, and the matrix element needed for Fermi's golden rule is given by

$$\mathcal{M}^{(\uparrow\downarrow)} = \frac{e}{m_p}\sqrt{\frac{2\pi\hbar}{\omega_\mathbf{k} V}}\left\langle(\uparrow\downarrow)p\pi^0\frac{\mathrm{e}^{i\mathbf{q}\cdot\mathbf{r}}}{\sqrt{V}}\frac{\mathrm{e}^{i\mathbf{Q}\cdot\mathbf{r}}}{\sqrt{V}}|\mathrm{e}^{i\mathbf{k}(\mathbf{R} - \frac{m_\pi}{M_{p\pi}}\mathbf{r})}(\mathbf{e}_{\mathbf{k},\lambda}\mathbf{p})|\psi_{N\pi}\right\rangle, \tag{4.55}$$

where $\mathbf{q}$ is the wave number of the relative pion-proton system and $\mathbf{Q} = \mathbf{k}$ is the recoil. Looking at the isospin coefficient from equation (3.4), which is the factor that separates neutral pions from charged pions aside from the mass difference[5]. Inserting (3.16) and using that volume condition yields the following expression[6]

5. $\left\langle p\pi^0\middle|\boldsymbol{\tau}\cdot\boldsymbol{\pi}\middle|p\right\rangle = 1$

6. $\int \mathrm{d}^3R\,\mathrm{e}^{i\mathbf{k}\cdot\mathbf{R}} = V$

$$\mathcal{M}^{(\uparrow\downarrow)} = \frac{e}{m_p}\sqrt{\frac{2\pi\hbar}{\omega_\mathbf{k} V}}\left\langle(\uparrow\downarrow)p\pi^0\frac{\mathrm{e}^{i\mathbf{q}\cdot\mathbf{r}}}{\sqrt{V}}|\mathrm{e}^{-i\frac{m_\pi}{M_{p\pi}}\mathbf{k}\cdot\mathbf{r}}(\mathbf{e}_{\mathbf{k},\lambda}\mathbf{p})|(\boldsymbol{\tau}\cdot\boldsymbol{\pi})(\boldsymbol{\sigma}\cdot\mathbf{r})\phi(r)\frac{p\uparrow}{\sqrt{V}}\right\rangle \tag{4.56}$$

Defining a new vector, $\mathbf{s} = \mathbf{q} + \frac{m_\pi}{M_{p\pi}}\mathbf{k}$ yields

$$\mathcal{M}^{(\uparrow\downarrow)} = \frac{-e}{m_\pi}\sqrt{\frac{2\pi\hbar}{\omega_\mathbf{k}}}\frac{1}{V}\left\langle(\uparrow\downarrow)\right|\left\langle\mathrm{e}^{is\cdot\mathbf{r}}|(\mathbf{e}_{\mathbf{k},\lambda}\mathbf{p})(\boldsymbol{\sigma}\cdot\mathbf{r})|\phi(r)\right\rangle\left|\uparrow\right\rangle \tag{4.57}$$

Note the different inner products. We now consider the innermost matrix element in equation (4.57) where the momentum operator is inserted

$$\left\langle\mathrm{e}^{is\cdot\mathbf{r}}|(\mathbf{e}_{\mathbf{k},\lambda}\frac{\partial}{\partial\mathbf{r}})(\boldsymbol{\sigma}\cdot\mathbf{r})|\phi(r)\right\rangle = +i(\mathbf{e}_{\mathbf{k},\lambda}\cdot\mathbf{s})\int \mathrm{d}^3r\,\mathrm{e}^{is\cdot\mathbf{r}}(\boldsymbol{\sigma}\cdot\mathbf{r})\phi(r) \tag{4.58}$$

$$= -i(\mathbf{e}_{\mathbf{k},\lambda}\cdot\mathbf{s})\int \mathrm{d}^3r\,3ij_1(sr)\frac{\mathbf{s}\cdot\mathbf{r}}{sr}(\boldsymbol{\sigma}\cdot\mathbf{r})\phi(r) \tag{4.59}$$

$$= (\mathbf{e}_{\mathbf{k},\lambda}\cdot\mathbf{s})(\boldsymbol{\sigma}\cdot\mathbf{r})\underbrace{\frac{4\pi}{s}\int_0^\infty \mathrm{d}r\,r^3 j_1(sr)\phi(r)}_{F(s)} \tag{4.60}$$

$$= (\mathbf{e}_{\mathbf{k},\lambda}\cdot\mathbf{s})(\boldsymbol{\sigma}\cdot\mathbf{r})F(s). \tag{4.61}$$

Where we used the spherical Bessel decomposition (B.9) in equation (4.59). In equation (4.60) we considered the angular averaging of two coordinates variables[7]. We now have an expression for the innermost matrix element in equation (4.57), which depends on the wave function $\phi(r)$. This is where the two parameters S and b enter, and ultimately these are the parameters we want to extract. Returning to the matrix element (4.57)

7. $\int \mathrm{d}\Omega\, n_k n_l = \frac{4\pi}{3}\delta_{kl}$, which means $\int \mathrm{d}\Omega\, r_k r_l = \frac{4\pi r^2}{3}\delta_{kl}$, where n is a unit vector.

$$\mathcal{M}^{(\uparrow\downarrow)} = \frac{ie\hbar}{m_p}\sqrt{\frac{2\pi\hbar}{\omega_k}}\frac{1}{V}\langle(\uparrow\downarrow)|(\mathbf{e}_{\mathbf{k},\lambda}\cdot\mathbf{s})F(s)|\uparrow\rangle \tag{4.62}$$

$$= \frac{ie\hbar}{m_p}\sqrt{\frac{2\pi\hbar}{\omega_k}}\frac{1}{V}(\mathbf{e}_{\mathbf{k},\lambda}\cdot\mathbf{s})\,\langle(\uparrow\downarrow)|(\boldsymbol{\sigma}\cdot\mathbf{r})|\uparrow\rangle\, F(s), \tag{4.63}$$

which leads to the following expression for the norm square of equation (4.57). We do this step already to use a completeness relation for the polarisation.

$$\left|\mathcal{M}^{(\uparrow\downarrow)}\right|^2 = \frac{2\pi\hbar^3 e^2}{m_p^2\omega_k V^2}\left|\mathbf{e}_{\mathbf{k},\lambda}\cdot\mathbf{s}\right|^2\left|\langle(\uparrow\downarrow)|(\boldsymbol{\sigma}\cdot\mathbf{s})|\uparrow\rangle\right|^2 F(s)^2, \tag{4.64}$$

and now calculating

$$\sum_\lambda\left|(\mathbf{e}_{\mathbf{k},\lambda}\cdot\mathbf{s})\right|^2 = \sum_\lambda(\mathbf{e}^*_{\mathbf{k},\lambda}\cdot\mathbf{s})(\mathbf{e}_{\mathbf{k},\lambda}\cdot\mathbf{s}) \tag{4.65}$$

$$= s^2 - \frac{(\mathbf{k}\cdot\mathbf{s})^2}{k^2} \tag{4.66}$$

$$= q^2 - \frac{(\mathbf{k}\cdot\mathbf{q})^2}{k^2} \tag{4.67}$$

$$= q^2\sin^2(\theta_q), \tag{4.68}$$

where θ_q is the angle between $\mathbf{k}$ and $\mathbf{q}$, and we now have an angular dependency originating from the dot product. This step also assumes the target is unpolarised since we sum over the spin states of the proton. The subscript q is used to emphasise that this is relative to the final state momentum, also mentioned in section 2.2. The final missing term is calculated by summing over the final proton spin states using (3.5)

$$\sum_{(\uparrow\downarrow)}\left|\langle(\uparrow\downarrow)|(\boldsymbol{\sigma}\cdot\mathbf{s})|\uparrow\rangle\right|^2 = s^2 \tag{4.69}$$

Using the final two expressions equation (4.68) and (4.69) with equation (4.64) and remembering the factor $1/2$ from the spin states

$$\frac{1}{2}\sum_{\lambda,(\uparrow\downarrow)}\left|\mathcal{M}_{fi}\right|^2 = \frac{\pi e^2\hbar^3}{V^2 m_p^2}\frac{1}{\omega_k}q^2\sin^2(\theta)s^2F(s)^2. \tag{4.70}$$

According to Fermi's golden rule, the transition probability is given by

$$\mathrm{d}\omega = \frac{2\pi}{\hbar}|\mathcal{M}|^2\,\mathrm{d}\rho, \tag{4.71}$$

where we can use both expressions for the density of states. We can either use the relativistic equation (2.18) or the non-relativistic equation (2.19). We will use the relativistic expression as an example but show both results at the end of the section. This leads to the final transition probability

$$\mathrm{d}\omega^0 = \frac{e^2c}{8\pi V}\frac{1}{m_p^2c^4}\frac{\mathrm{d}(\hbar cq)^2}{\mathrm{d}E_q}\frac{q^3}{k}\sin^2(\theta_q)s^2F(s)^2\mathrm{d}\Omega_q \tag{4.72}$$

which leads to the following expression for the differential cross section by considering the time it takes the photon to cross the volume, V.

$$\frac{d\sigma^0(E_q,\theta_q)}{d\Omega_q} = \frac{e^2}{8\pi}\frac{1}{m_p^2c^4}\frac{q^3}{k}\frac{d(\hbar cq)^2}{dE_q}\sin^2(\theta_q)s^2F(s)^2, \tag{4.73}$$

where the superscript is used to indicate the photoproduction of neutral pions. To get the total cross-section, we integrate all angles

$$\sigma^0 = 2\pi\int_0^\pi d\theta_q\ \sin(\theta_q)\frac{d\sigma^0}{d\Omega_q} \tag{4.74}$$

$$= 2\pi\int_0^\pi d\theta_q\frac{e^2}{8\pi}\frac{1}{m_p^2c^4}\frac{q^3}{k}\frac{d(\hbar cq)^2}{dE_q}\sin^3(\theta_q)s^2F(s)^2. \tag{4.75}$$

Equation (4.75) might seem easy to calculate at first, but we have to remember $F(s)$ also contains an angular dependency originating from the magnitude of **s**. We now perform a fit of equation (4.75) to experimental data for the parameters S and b. This is shown in figure 4.6 for the relativistic density of states. Data is from [13].

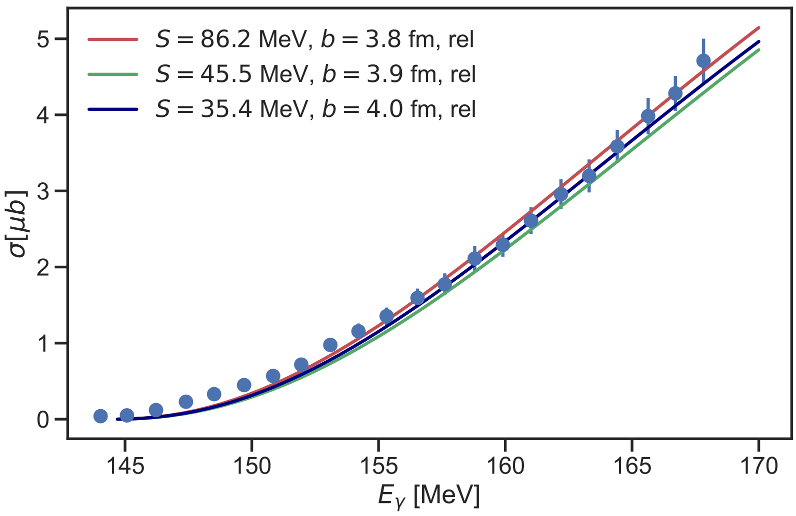

Figure 4.6: Fitted parameters to experimental data for the process $\gamma p \longrightarrow \pi^0 p$ using the relativistic density of states (2.18). The fit parameters for S, b are shown inside the figure. Data is from [13]

We see that the model with explicit pions can reproduce experimental data for at least three sets of parameters. The same figure can be reproduced for the non-relativistic density of states (2.19) where the total cross section is given by

$$\sigma^0 = 2\pi\int_0^\pi d\theta_q\frac{e^2}{4\pi}\frac{\mu_{p\pi}c^2}{m_p^2c^4}\frac{q^3}{k}\sin^3(\theta_q)s^2F(s)^2. \tag{4.76}$$

This is shown in figure 4.7

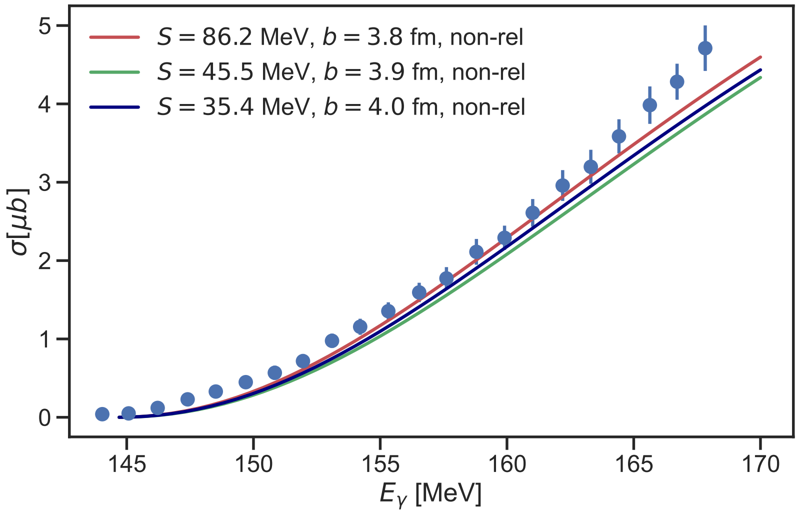

Figure 4.7: The same parameters as in figure 4.6 but using the non-relativistic density of states (2.19).

The total cross-section falls off too quickly as relativistic effects become more important. In equation (4.73), we have an expression for the angular dependency. This means that for some photon energy, we get an angular distribution. Figure 4.8 shows the differential cross section as a function of the angle θ_q compared to experimental data. Data is from [1]

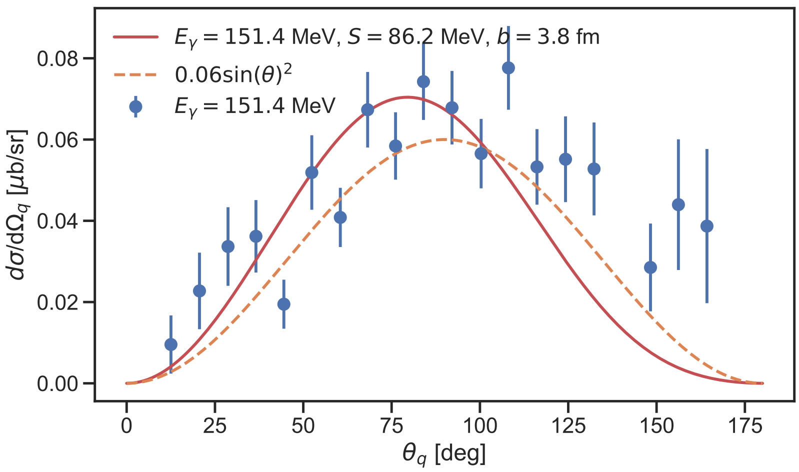

Figure 4.8: Angular distribution using equation (4.73) and experimental data from [1]. Note the dependency is not $\sin(\theta_q)^2$ since there is a contribution from $F(s)$ as well.

Figure 4.8 also shows how the angular dependency is not a $\sin(\theta_q)^2$ but also has some contribution from $F(s)$. Figure 4.9 shows multiple different photon energies.

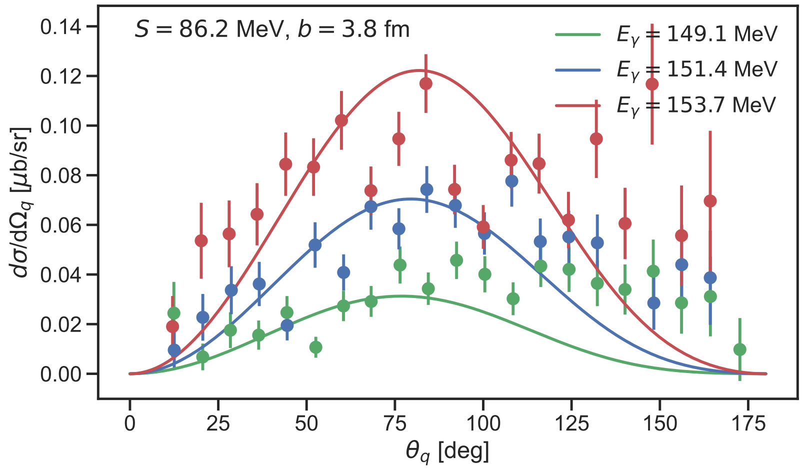

Figure 4.9: Angular distribution and experimental data for three different energies. Data is from [1]

Figures for the differential cross-section using different parameters and using the non-relativistic density of states are shown in appendix D.

The final thing we need to consider is the relative weight of the π^0 component in the wave function of the dressed proton. As in section 4.1, it is calculated as

$$C(\psi_{N\pi^0}) = \int_V \mathrm{d}^3R \int_V \mathrm{d}^3r \left|\psi_{N\pi}\right|^2 = 4\pi \int_0^\infty \mathrm{d}r\, \phi(r)^2 r^4 \tag{4.77}$$

For the three sets of parameters shown in figure 4.6, the contribution to the wave function from the π^0 is

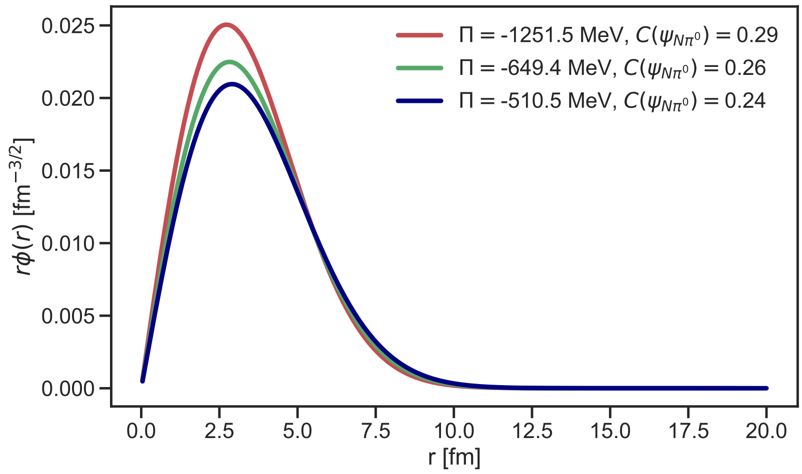

Figure 4.10: Radial wave functions using the parameters shown figure 4.6. Also includes virtual pions contribution to the dressed proton and the relative weight of the π^0 component in the wave function.

The contribution to the total wave function is, in principle, the relative weight of the two-component wave function in equation (3.1). We now know for a given set of parameters how much the pion-nucleon system contributes to the total wave function, and this can be related to something observable. The two-component wave function contains the wave function $\psi_{N\pi}(\mathbf{r}_\pi, \mathbf{r}_N)$, which is a two-dimensional position wave function. This is means the probability density in a volume $\mathrm{d}\mathbf{r}_\pi\, \mathrm{d}\mathbf{r}_p$ at position $(\mathbf{r}_\pi, \mathbf{r}_p)$ is given by

$$\rho(\mathbf{r}_\pi, \mathbf{r}_p) = \left|\psi_{N\pi}(\mathbf{r}_\pi, \mathbf{r}_p)\right|^2, \tag{4.78}$$

and the probability of finding the pion at position $\mathbf{r}_\pi$ is then

$$\rho_\pi(\mathbf{r}_\pi) = \int \mathrm{d}\mathbf{r}_p \left|\psi(\mathbf{r}_\pi, \mathbf{r}_p)\right|^2, \tag{4.79}$$

where we now omit the index and remind ourselves that the radial wave function is given by $\psi = r\phi$ from section 3.4. This leads to the following expression for the total charge density of the pion-nucleon system

$$\rho(\mathbf{r}) = q_\pi \int \mathrm{d}\mathbf{r}_\pi \mathrm{d}\mathbf{r}_p \left|\psi(\mathbf{r}_\pi, \mathbf{r}_p)\right|^2 + q_p \int \mathrm{d}\mathbf{r}_\pi \mathrm{d}\mathbf{r}_p \left|\psi(\mathbf{r}_\pi, \mathbf{r}_p)\right|^2, \quad (4.80)$$

where q_π and q_p are the charge of the pion and the proton, respectively. We now calculate the two integrals in the center of mass using the relative coordinates illustrated in figure 4.5.

$$\rho_\pi(\mathbf{r}_{\mathrm{cm}}) = q_\pi \int \mathrm{d}\mathbf{r}_\pi \mathrm{d}\mathbf{r}_p \left|\psi(\mathbf{r}_\pi, \mathbf{r}_p)\right|^2 \delta(\mathbf{r}_\pi - \mathbf{R}, \mathbf{r}_{\mathrm{cm}}) \quad (4.81)$$

$$= q_\pi \int \mathrm{d}\mathbf{r}\,\mathrm{d}\mathbf{R} \left|\mathbf{r}\phi\left(\mathbf{R} + \frac{m_p}{M_{p\pi}}\mathbf{r}, \mathbf{R} - \frac{m_\pi}{M_{p\pi}}\right)\right|^2 \delta(\mathbf{R} + \frac{m_p}{M_{p\pi}}\mathbf{r} - \mathbf{R}, \mathbf{r}_{\mathrm{cm}}) \quad (4.82)$$

$$= q_\pi \left|\frac{M_{p\pi}}{m_p}\mathbf{r}_{\mathrm{cm}}\phi\left(\frac{M_{p\pi}}{m_p}\mathbf{r}_{\mathrm{cm}}\right)\right|^2. \quad (4.83)$$

The charge density can be calculated in a similar manner. This means we can plot equation (4.80), which is shown in figure 4.11 as a function of the absolute radius from the center of mass.

Figure 4.11: Charge density for the parameters S = 45.5 MeV and b = 3.9 fm.

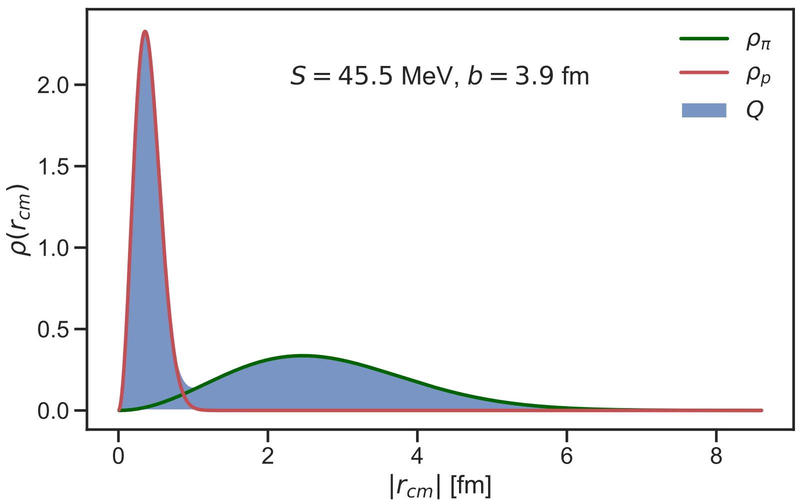

To complete the picture using the two-component wave function (3.1), we can imagine the bare proton as a delta function at $\mathbf{r}_{\mathrm{cm}} = 0$ and the probability density of the proton in the pion-nucleon system moved a distance to the left on the figure. The distance corresponds to the distance away from the center of mass due to the mass difference between the proton and the pion.

This also concludes the treatment of neutral pion photoproduction off protons. This section described the general framework of how to calculate the total cross-section and the charge density. These two observables are shown in figure 4.6 and figure 4.11, respectively.

4.2.2 Neutral Pion Photoproduction off Neutrons

Having considered neutral pions off protons, we now consider the closely related neutral pions off neutrons,

$$n\gamma \longrightarrow \pi^0 n, \quad (4.84)$$

The key difference is that now the pion is responsible for the interaction with the electromagnetic field, and hence equation (2.7) depends on the pion, which yields the following expression

$$H^{(1)} = -\frac{e}{m_\pi c}\mathbf{A}(\mathbf{r}_\pi, t) \cdot \mathbf{p}_\pi. \tag{4.85}$$

This changes two things in comparison to equation (4.73). The mass of the proton becomes the mass of the pion, and the wave number vector becomes $\mathbf{s} = \mathbf{q} - \frac{m_n}{M_{n\pi}}\mathbf{k}$, where m_n is the mass of the neutron. Therefore the final expression for the total cross-section becomes

$$\frac{\mathrm{d}\sigma^0(E_q, \theta_q)}{\mathrm{d}\Omega_q} = \frac{e^2}{8\pi}\frac{1}{m_\pi^2 c^4}\frac{q^3}{k}\frac{\mathrm{d}(\hbar c q)^2}{\mathrm{d}E_q}\sin^2(\theta_q)s^2 F(s)^2. \tag{4.86}$$

Unfortunately, no experimental data exists such that a fit can be performed. Due to the similarities between the proton and the neutron, one could expect experimental data similar to 4.6, which would mean different fit parameters since the pion is now responsible for the interaction with the electromagnetic field. Figure 4.12 shows the total cross-section for the process in equation (4.86) using the same fit parameters as in the previous section. The dashed lines are made using the non-relativistic density of states.

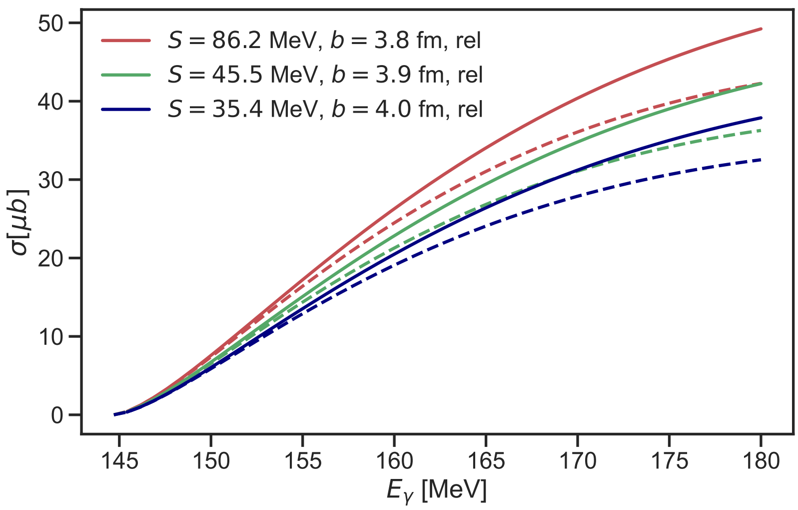

Figure 4.12: The process $\gamma n \longrightarrow \pi^0 n$ with the same parameters as for neutral pion photoproduction off protons.

4.2.3 Charged Pion Photoproduction off Protons

Moving on to charged pions, we first consider the following process,

$$p\gamma \longrightarrow \pi^+ n, \tag{4.87}$$

where charged pions are generated off the proton. Note that the charged pion is different in two ways compared to the neutral pion. The mass is approximately 5 MeV higher, and it contains an isospin coefficient from (3.4), which means we get the following extra contribution

$$\langle n\pi^+|\boldsymbol{\tau} \cdot \boldsymbol{\pi}|p\rangle = \sqrt{2}. \tag{4.88}$$

Carrying this factor through the calculations in section 4.2.1 amounts to a factor 2. This means the total cross-section is given by

$$\sigma^+ = 2\pi \int_0^\pi \mathrm{d}\theta_q \frac{e^2}{4\pi}\frac{1}{m_p^2 c^4}\frac{q^3}{k}\frac{\mathrm{d}(\hbar c q)^2}{\mathrm{d}E_q}\sin^3(\theta_q)s^2 F(s)^2, \tag{4.89}$$

where the + indicates the production of positively charged pions. We once again fit equation (4.89) to experimental data. The result can be seen in figure 4.13, where the data is from

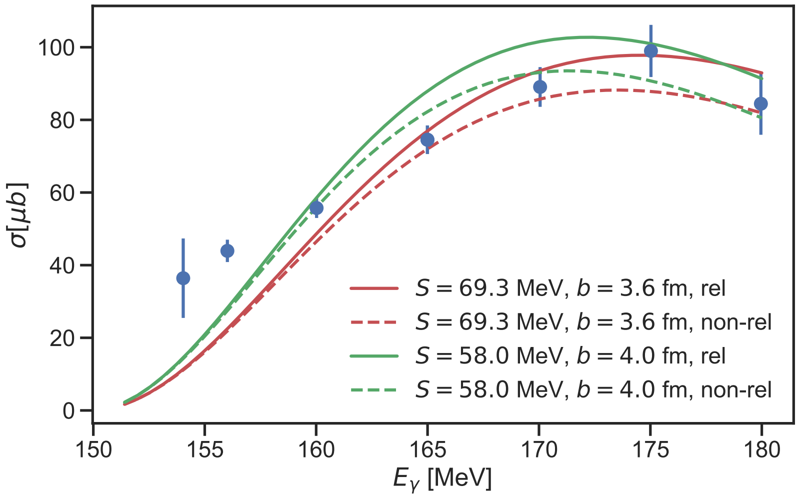

Figure 4.13: Fitted parameters shown inside the figure. The dashed lines are made using the non-relativistic density of states (2.19). Data from [3]

Figure 4.13 shows the model has difficulty accurately describing the pion photoproduction of charged pions. The data points near the threshold cannot adequately be described by the parameters shown in the figure. This can be explained by the spherical Bessel function $j_1(sr)$ in the integral $F(s)$ in equation (4.89). The spherical Bessel function is 0 for $s = 0$, which means the data points near the threshold can only be included if the integral is much higher. There is a trade-off since the r^3 dependency begins to dominate the integral. This means the data points near the threshold can be better described by the $j_0(qr)$ as in the dipole approximation. A combined plot is shown in figure 4.14.

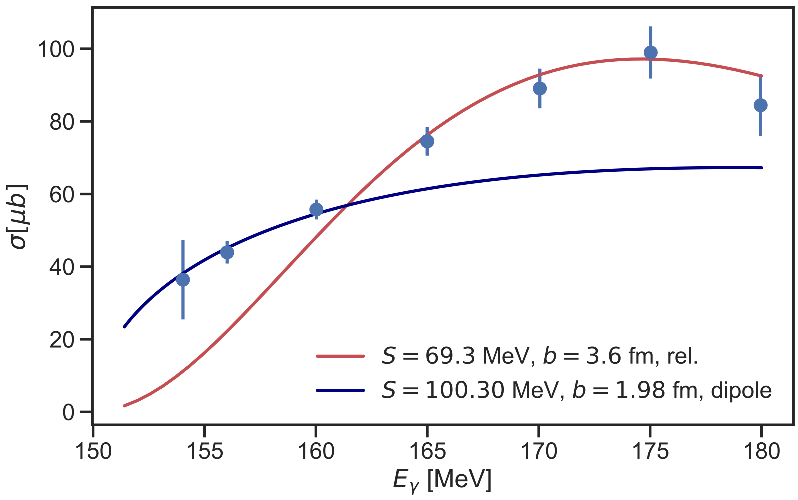

Figure 4.14: Best fit using both the dipole approximation for data points near the threshold and the exact approach for energies where the dipole approximation is no longer valid.

We now focus on the weight of the π^+ component in the wave function and the pions contribution to the mass of the dressed proton. This is shown in figure 4.15 where the colours match from figure 4.13 and figure 4.14

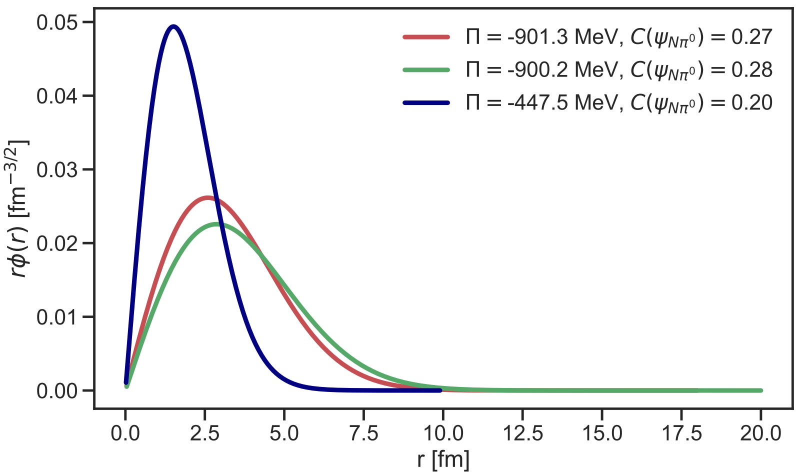

Figure 4.15: Radial wave functions using the parameters shown figure 4.13 and figure 4.14. Also includes virtual pions contribution to the dressed proton and the relative weight of the π^- component in the wave function

The energy is much lower when considering the parameters from the dipole approximation. The contributions are similar, which is impressive considering a difference of $S \sim 40$ MeV and $b \sim 2$ fm in the parameters.

4.2.4 Charged Pion Photoproduction off Neutrons

The last process to be investigated involves charged pions off a neutron,

$$n\gamma \longrightarrow \pi^- p, \tag{4.90}$$

which is also the most complicated since there is a Coulomb interaction between the two particles in the final state. Ignoring this temporarily and we can deduce the expression for the total cross-section by combining the effects from section 4.2.2 and section 4.2.3. This means an isospin coefficient from

$$\langle p\pi^- | \boldsymbol{\tau} \cdot \boldsymbol{\pi} | n \rangle = \sqrt{2}, \tag{4.91}$$

and the mass of the pion in the denominator since the pion is responsible for the interaction with the electromagnetic field. Therefore the total cross-section is given by

$$\sigma^- = 2\pi \int_0^\pi \mathrm{d}\theta_q \, \frac{e^2}{4\pi} \frac{1}{m_\pi^2 c^4} \frac{q^3}{k} \frac{\mathrm{d}(\hbar c q)^2}{\mathrm{d}E_q} \sin^3(\theta_q) s^2 F(s)^2. \tag{4.92}$$

However, the integral $F(s)$ is different since we have to account for the Coulomb interaction between the two charged particles in the final state. The behaviour of the charged particles can be described by an attractive Coulomb wave function, $F_\ell(\eta, kr)$. This is covered in appendix B.3. This leads to the final expression for the total cross-section using the regular Coulomb wave functions

$$\sigma^- = \int_0^\pi \mathrm{d}\theta_q \, \frac{e^2}{2} \frac{1}{m_\pi^2 c^4} \frac{q^3}{k} \frac{\mathrm{d}(\hbar c q)^2}{\mathrm{d}E_q} \sin^3(\theta_q) s^2 \left(\frac{4\pi}{s} \int_0^\infty \mathrm{d}r \, F_1(\eta, sr) r^3 \phi(r) \right)^2, \tag{4.93}$$

where η is the parameter that determines the strength of the Coulomb interaction given by

$$\eta = \frac{Z \mu_{p\pi} c \alpha}{\hbar k}. \tag{4.94}$$

Here Z is the product of the charges. Letting this parameter be equal to zero will reduce the Coulomb wave function to a spherical Bessel function.

Chapter 5

Conclusion

In this thesis, we set out to investigate pion photoproduction in a nuclear model with explicit mesons. To do this we first introduced the model in section 3 and considered how a general system can be investigated. We then focused on the dressing of the proton specifically and introduced a method of solving the wave function numerically. We when exploited the generality of the model to consider different form factors and how this affected the solutions. We also considered a different operator type which is more related to the operator found in effective field theories. This model turned out to be similar but also a lot more intensive numerically.

Bibliography

[1] R. Beck, F. Kalleicher, B. Schoch, J. Vogt, G. Koch, H. Ströher, V. Metag, J. C. McGeorge, J. D. Kellie, and S. J. Hall. Measurement of the p(γ,π^0) cross section at threshold. *Phys. Rev. Lett.*, 65: 1841–1844, Oct 1990. doi: 10.1103/PhysRevLett.65.1841. URL `https://link.aps.org/doi/10.1103/PhysRevLett.65.1841`.

[2] Blatt and Weisskopf. *Theoretical Nuclear Physics*. Springer, New York, NY, first edition, 1958.

[3] W. Briscoe, A. Kudryavtsev, I. Strakovsky, V. E. V.E. Tarasov, and R. Workman. Threshold π^- photoproduction on the neutron. *The European Physical Journal A*, 56(218), 2020. doi: https://doi.org/10.1140/epja/s10050-020-00221-w.

[4] DLMF. *NIST Digital Library of Mathematical Functions*. http://dlmf.nist.gov/, Release 1.1.7 of 2022-10-15. URL `http://dlmf.nist.gov/`. F. W. J. Olver, A. B. Olde Daalhuis, D. W. Lozier, B. I. Schneider, R. F. Boisvert, C. W. Clark, B. R. Miller, B. V. Saunders, H. S. Cohl, and M. A. McClain, eds.

[5] D. V. Fedorov. A nuclear model with explicit mesons. *Few-Body Systems*, 61(4):40, October 2020. doi: 10.1007/s00601-020-01573-1. URL `https://doi.org/10.1007/s00601-020-01573-1`.

[6] D. V. Fedorov. A nuclear model with explicit mesons. *Few-Body Systems*, 61(4), Oct 2020. ISSN 1432-5411. doi: 10.1007/s00601-020-01573-1. URL `http://dx.doi.org/10.1007/s00601-020-01573-1`.

[7] D. V. Fedorov and M. Mikkelsen. Threshold photoproduction of neutral pions off protons in nuclear model with explicit mesons. 2022. doi: 10.48550/ARXIV.2209.12071. URL `https://arxiv.org/abs/2209.12071`.

[8] H. W. Hammer, S. König, and U. van Kolck. Nuclear effective field theory: status and perspectives. 2019. doi: 10.48550/ARXIV.1906.12122. URL `https://arxiv.org/abs/1906.12122`.

[9] J. D. Jackson. *Classical Electrodynamics*. Wiley, 3rd edition edition, 1999.

[10] B. R. Martin and G. Shaw. *Nuclear and Particle Physics: An Introduction*. Wiley, 3rd edition, 2019.

[11] G. A. Miller. The fundamental nature of low-energy pion-nucleon interactions, 2022. URL `https://arxiv.org/abs/2208.12873`.

[12] J. J. Sakurai and J. Napolitano. *Modern Quantum Mechanics*. Cambridge University Press, 2nd edition, 2017.

[13] A. Schmidt, P. Achenbach, J. Ahrens, H. J. Arends, R. Beck, A. M. Bernstein, V. Hejny, M. Kotulla, B. Krusche, V. Kuhr, R. Leukel, I. J. D. MacGregor, J. C. McGeorge, V. Metag, V. M. Olmos de León, F. Rambo, U. Siodlaczek, H. Ströher, T. Walcher, J. Weiß, F. Wissmann, and M. Wolf. Test of low-energy theorems for ${}^1h(\vec{\gamma}, \pi^0)^1h$ in the threshold region. *Phys. Rev. Lett.*, 87:232501, Nov 2001. doi: 10.1103/PhysRevLett.87.232501. URL https://link.aps.org/doi/10.1103/PhysRevLett.87.232501.

[14] P. Siemens and A. Jensen. *Elements of Nuclei: Many-Body Physics with the Strong Interaction*. CRC Press, 03 2018. ISBN 9780429493904. doi: 10.1201/9780429493904.

[15] A. V. Zee. Group theory in a nutshell for physicists. Princeton University Press, 2016. ISBN 9780691162690.

[16] V. Zelevinsky and A. Volya. *Physics of Atomic Nuclei*. Wiley-VCH, first edition, 2017.

Appendix A

Nuclear photoeffect and the deuteron

In this appendix, we go through how to get expressions for the differential cross-section and the total cross-section from the wave function. The wave function can be obtained analytically or numerically. In this appendix, we will sketch an analytical approach to s-wave calculations. Considering the central potential between the proton and the neutron given by

$$U(r) = \begin{cases} -U_0, & r \leq R \\ 0 & r > R, \end{cases}$$

the radial equation is given by

$$-\frac{\hbar^2}{2m}\frac{\mathrm{d}^2 u(r)}{\mathrm{d}r^2} + \left[U(r) + \frac{\hbar^2 \ell(\ell+1)}{2mr^2}\right] u(r) = Eu(r). \tag{A.1}$$

This is identical to the one-dimensional Schrödinger equation with an effective potential, where the centrifugal term pushes the particle outwards. To solve this analytically, we rewrite the equation and consider the boundary conditions.

$$\frac{\mathrm{d}^2 u(r)}{\mathrm{d}r^2} + \frac{M}{\hbar^2}\left[E - U(r)\right] u(r) = 0, \tag{A.2}$$

where we plugged in the expression for the reduced mass, $m = M/2$. For the deuteron, we use $E = -E_B = -2.225$ MeV [16]. This leads to the following expressions

$$\frac{\mathrm{d}^2 u(r)}{\mathrm{d}r^2} + \frac{M}{\hbar^2}\left(U_0 - E_B\right) u(r) = 0, \quad r \leq R, \tag{A.3}$$

$$\frac{\mathrm{d}^2 u(r)}{\mathrm{d}r^2} - \frac{M}{\hbar^2} E_B u(r) = 0, \quad r > R. \tag{A.4}$$

We introduce two variables given by

$$k = \sqrt{\frac{M}{\hbar^2}\left(U_0 - E_B\right)}, \quad \kappa = \sqrt{\frac{ME_B}{\hbar^2}}. \tag{A.5}$$

Rewriting equation (A.3) in terms of (A.5) and solving the differential equation yields

$$\frac{\mathrm{d}^2 u(r)}{\mathrm{d}r^2} = -ku(r) \Rightarrow u(r) = A\sin(kr) + B\cos(kr). \tag{A.6}$$

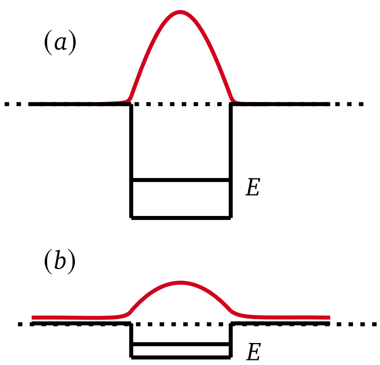

Figure A.1: Behavior of the ground state bound wave function for two potentials. (a) is an illustration of the deeper potential well case and (b) is for a shallower potential well.

Since $R(r) = u(r)/r$ and $\cos(kr)/r$ blows up as $r \to 0 \Rightarrow B = 0$ and the solution is

$$u(r) = A\sin(kr), \quad r \leq R \tag{A.7}$$

Now, considering equation (A.4)

$$\frac{\mathrm{d}^2 u(r)}{\mathrm{d}r^2} = \kappa^2 u(r) \Rightarrow u(r) = Ce^{\kappa r} + De^{-\kappa r} \tag{A.8}$$

Here $Ce^{\kappa r}$ blows up as $r \to \infty$. The wavefunction must be continuous, and this means the solutions (A.6) and (A.8) must match at $r = R$. The same applies to the derivative. This leads to two equations for $r = R$.

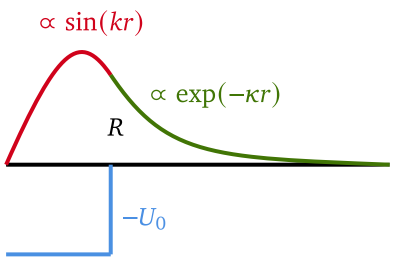

Figure A.2: The s-wave wave function for the deuteron.

$$A\sin(kR) = De^{-\kappa R} \tag{A.9}$$

$$Ak\cos(kR) = -D\kappa e^{-\kappa R} \tag{A.10}$$

Dividing equation (A.10) by equation (A.9) leads to

$$-\cot(kR) = \frac{\kappa}{k} \tag{A.11}$$

This equation is solved by requiring $kR = \pi/2$. Plugging in an appropriate value for $R = 1.7$ fm yields

$$\begin{aligned} U_0 &= \frac{\hbar^2\pi^2}{2mR^2} - E \\ &= \frac{\hbar^2\pi^2}{2mR^2} + E_B \\ &= 37.2\,\mathrm{MeV} \end{aligned}$$

	0^+	0^-	1^+	1^-
Singlet	$^1s_0$			$^1p_1$
Triplet		3^p_0	$^3s_1, ^3d_1$	$^3p_1$

Table A.1: Two nucleon states J^Π. The deuteron consists of a wave function superposition of $^3s_1 + ^3d_1$.

This means the depth of the potential is 37.2 MeV.

Note that this is all for s-wave. Some considerations about the tensor force are also needed. This means we have to consider the Schrödinger equation with noncentral spin-dependent potential given by

$$\mathcal{U}(r) = \mathcal{U}_0(r) + \mathcal{U}_t(r)S_{12}, \tag{A.12}$$

where

$$\mathcal{U}_t(r) = \mathcal{U}_{tW}(r) + \mathcal{U}_{tM}(r), \tag{A.13}$$

for the space-even states we are considering with the deuteron, see table A. Considering the d-wave we introduce the angular momentum coupling $[Y_2(\mathbf{n})\chi_1]_{1M}$ of spin 1 and $\ell = 1$ to the total deuteron spin $J = 1$ and projection $J_z = M$. The same coupling but properly normalized can be written as

$$\Theta_M = \frac{1}{\sqrt{32\pi}} S_{12}\chi_{1M}. \tag{A.14}$$

To get the complete wave function of the deuteron, the expression must contain two radial parts and a spherical wave factor $1/r$

$$\Psi_M = \frac{1}{\sqrt{4\pi}}\frac{1}{r}\left(u_0(r) + \frac{1}{\sqrt{8}}u_2(r)S_{12}\right)\chi_{1M}, \tag{A.15}$$

where the two radial parts are $u_0(r)$ and $u_2(r)$ for s-wave and d-wave respectively. These must also be normalized as

$$\int_0^\infty \mathrm{d}r\,|u_0|^2 + \int_0^\infty \mathrm{d}r\,|u_2|^2 = 1. \tag{A.16}$$

Moreover, the two terms can be interpreted as a weight for the respective wave. Now using the expression for the deuteron wave function equation

(A.15) we want to get an expression for the differential cross section for the nuclear photoeffect. When an absorbed photon frequency exceeds the lowest threshold of nuclear decay, the nucleus becomes excited to the continuum states. We consider the case where the decay happens through particle emission. In other words, this is the absorption of a photon that results in particle decay into the continuum. From the conservation of energy, we have

$$E_i = \hbar\omega = E_f + \epsilon, \tag{A.17}$$

where the nucleus A goes from the initial state with energy E_i to the final state with $A-1$ and energy E_f and the particle in the continuum has energy $\epsilon = \mathbf{p}^2/2m$.

The excitation of the discrete states that show resonance behaviour, and the continuum of energy states makes for a more smooth dependence. This means we can use what we know from the discrete excitation but introduce a level density ρ_f instead of the usual delta function in the expression for the differential cross section. This yields

$$\mathrm{d}\sigma_{fi} = \frac{4\pi^2\hbar}{E_\gamma c}\left|\sum_a \frac{\mathbf{e_a}}{m_a}\left\langle f\middle|(\mathbf{p}_a\cdot\mathbf{e}_{\mathbf{k}\lambda})\mathrm{e}^{i(\mathbf{k}\cdot\mathbf{r}_a)}\middle|i\right\rangle\right|^2\rho_f, \tag{A.18}$$

where the level density is given by

$$\rho_f = \frac{Vmp}{(2\pi\hbar)^3}\mathrm{d}o. \tag{A.19}$$

Here the particle is emitted with momentum $\mathbf{p}$ into the solid angle element do, and E_γ is the energy of the photon. In the case of the deuteron equation (A.18) and be split into different multipolarities. The most simple is the electric dipole transition ($E1$).

In the long wavelength limit the plane wave expression reduces to unity, which means equation (A.18) for the dipole transition can be written as

$$\mathrm{d}\sigma_{E1} = \frac{\alpha m p\omega}{\hbar^2}\left|\sum_a(\mathbf{e}\cdot\mathbf{r_a})_{fi}\right|^2\frac{\mathrm{d}o}{4\pi}, \tag{A.20}$$

where the solid angle could be the direction along the motion of the proton[1].

When assuming an unpolarized deuteron, we can take the average over the spin states $1/3\sum_m$ and count all final polarizations $\sum_{m'}$[2]. The final state is still spin triplet since the dipole operator does not act on the spin variable. This yields

$$\overline{\mathrm{d}\sigma_{E1}} = \frac{1}{4}\frac{\alpha m p\omega}{\hbar^2}\frac{1}{3}\sum_{mm'}\left|(\mathbf{e}\cdot\mathbf{r})_{fi}\right|^2\frac{\mathrm{d}o}{4\pi}. \tag{A.21}$$

The task is now to find an expression for the dot product in the sum. After the $E1$ transition, the final spin state remains a triplet with $S = J = 1$; the orbital and parity, however, are not the same. The final state corresponds to the p-wave, where the low-energy nuclear forces are weak, and the wavelength of the relative motion is much larger than the range of those forces. From conservation of energy, we have

$$\frac{\hbar^2k^2}{2m} = \hbar\omega - \epsilon. \tag{A.22}$$

For any direction of the relative momentum vector $\hbar\mathbf{k}$ the p-wave component must be normalized through some Legendre polynomial $P_1(\cos(\theta))$ and the spherical Bessel function $j_{\ell=1}(kr)$.[3]

1. Also, $V = 1$ and $\alpha = e^2/\hbar c$

2. Note m and m'

3. $P_1(\cos(\theta)) = \cos(\theta)$ and $j_1(\rho) = \frac{\sin(\rho)-\rho\cos(\rho)}{\rho^2}$.

Here θ is the angle between the relative coordinate $\mathbf{r}$ and the wave vector $\mathbf{k}$ this yields

$$\psi_f(r,\theta) = 3i\cos(\theta) j_1(kr)\chi_{mm'} \tag{A.23}$$

In the s-wave transition, we get the following expression when integration over the angles of the unit vector $\mathbf{n} = \mathbf{r}/r$

$$\frac{1}{2}\left\langle f;m'\middle|(\mathbf{e}\cdot\mathbf{r})\middle|\ell=0;m\right\rangle = -i\frac{\sqrt{\pi}}{k}(\mathbf{e}\cdot\mathbf{k})I_0\delta_{mm'}. \tag{A.24}$$

The radial integrals for the s-wave and d-wave are given by I_0 and I_2 respectively.[4] For the d-wave we have to reintroduce the tensor operator[5] S_12. Just like in the s-wave case, we have to integrate over the unit vector – this time, however, it contains four components

4. $I_\ell = \int_0^\infty \mathrm{d}r\, r^2 j_1(kr)u_\ell(r)$, $\ell = 0, 2$

5.

$$S_{12}(\mathbf{n}) = 3(\boldsymbol{\sigma}_1\cdot\mathbf{n})(\boldsymbol{\sigma}_2)\cdot\mathbf{n} - (\boldsymbol{\sigma}_1\cdot\boldsymbol{\sigma}_2) = 2[3(\mathbf{S}\cdot\mathbf{n})^2 - \mathbf{S}^2]$$

$$\int \mathrm{d}o\, n_i n_j n_k n_l = \frac{4\pi}{15}(\delta ij\delta_{kl} + \delta_{ik}\delta_{jl} + \delta_{il}\delta_{jk}), \tag{A.25}$$

and the d-wave contribution is given by

$$\frac{1}{2}\left\langle f;m'\middle|(\mathbf{e}\cdot\mathbf{r})\middle|\ell=2;m\right\rangle = -i\frac{\sqrt{\pi}}{k}C_{m'm}I_2, \tag{A.26}$$

where the spin matrix element $C_{mm'}$ contains

$$C = \frac{2\sqrt{2}}{5}\left[\frac{3}{4}\left[(\mathbf{k}\cdot\mathbf{S})(\mathbf{e}\cdot\mathbf{S}) + (\mathbf{e}\cdot\mathbf{S})(\mathbf{k}\cdot\mathbf{S})\right] - (\mathbf{e}\cdot\mathbf{k})\right]. \tag{A.27}$$

Equation (A.27) can be rewritten using a trace identity[6] Skipping the calculation and moving back to equation (A.21), we have

6.

$$\sum_{mm'}|O_{m'm}|^2 = \sum_m (O^\dagger O)_{mm} = \mathrm{Tr}\{O^\dagger O\}$$

$$\frac{1}{3}\sum_{mm'}\left|(\mathbf{e}\cdot\mathbf{r})_{fi}\right|^2 = 4\pi\left(I_0^2\cos^2(\alpha) + \frac{1}{25}I_2^2(3+\cos^2(\alpha))\right), \tag{A.28}$$

where α is the angle between $\mathbf{e}$ and the momentum of the final nucleon $\mathbf{k}$. The final steps involve averaging over the transverse polarizations of the initial photon, which also relates the angle α to the experimentally observed angle between the directions of the photon and final nucleus. This means we get the following expression

$$\overline{\cos^2(\alpha)} = \frac{1}{2}\sin^2(\theta) \tag{A.29}$$

Plugging this into equation (A.20) yields

$$\mathrm{d}\sigma_{E1} = \frac{\pi}{2}\frac{\alpha m p\omega}{\hbar^2}\left[I_0^2\sin^2(\theta) + \frac{1}{25}(6+\sin^2(\theta))I_2^2\right]\frac{\mathrm{d}o}{4\pi}, \tag{A.30}$$

and we arrive at the final expression when integrating over the angle of emitted photons

$$\sigma_{E1} = \frac{\pi}{3}\frac{\alpha m p\omega}{\hbar^2}\left(I_0^2 + \frac{2}{5}I_2^2\right). \tag{A.31}$$

It is also possible to estimate the cross-section in equation (A.31) using the initial wave function of the approximation of weak binding. Here the wave function is replaced by its exponential tail outside the range of nuclear forces. Furthermore, the contribution I_2 is neglected. This means the wave function is given by

$$\psi_i = \sqrt{\frac{\kappa}{2\pi}}\frac{\mathrm{e}^{-\kappa r}}{r}, \tag{A.32}$$

where κ is defined in equation (A.5). Calculating the integral I_0 yields

$$\sigma = \frac{8\pi}{3}\frac{\alpha\hbar^2}{M}\frac{\sqrt{\epsilon}(\hbar\omega - \epsilon)^{3/2}}{(\hbar\omega)^3}, \tag{A.33}$$

which is rewritten in terms of the photon energy, $\xi = \hbar\omega/\epsilon$ and in terms of numerical estimates

$$\sigma(\xi) \simeq 1.2\frac{(\xi - 1)^{3/2}}{\xi^3} \times 10^{-26}\,\mathrm{cm}^2. \tag{A.34}$$

The total cross-section of deuteron photodisintegration is shown in figure A.3

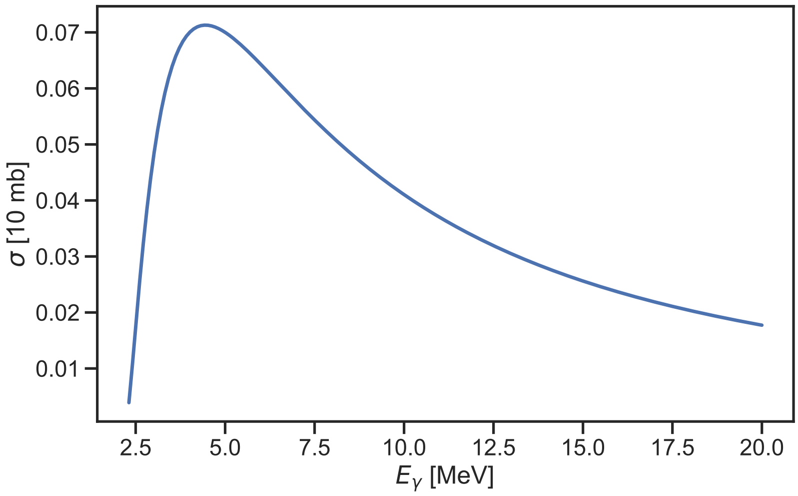

Figure A.3: Total cross section of deuteron photodisintegration as a function of photon energy divided by binding energy

Appendix **B**

Special functions and properties

This appendix covers the basics of some of the special functions that arise when discussing the properties of some operators in quantum mechanics and formulae used.

B.1 Legendre polynomials and spherical Bessel functions

$$Y_\ell^m(\theta,\phi) = \frac{(-1)^{\ell l+m}}{(2\ell)!!}\left[\frac{(2\ell+1)(\ell-m)}{4\pi(\ell+m)!}\right](\sin\theta)^m \frac{\mathrm{d}^{\ell+m}}{(d\cos\theta)^{\ell+m}}\left[(\sin\theta)^{2\ell}\right]\exp\{im\phi\}, \tag{B.1}$$

which satisfy

$$Y_\ell^{*m} = (-1)^m Y_l^{-m}. \tag{B.2}$$

The spherical harmonics are connected to the Legendre polynomials

$$P_\ell(\cos\theta) = \left[\frac{4\pi}{2\ell+1}\right]^{1/2} Y_l^0(\theta). \tag{B.3}$$

Another important feature of spherical harmonics is that they form a complete set of functions over the unit sphere. Furthermore, they form an orthonormal set

$$\int \mathrm{d}\Omega\, Y_\ell^{*m} Y_{l'}^{m'} = \delta_{mm'}\delta_{ll'}. \tag{B.4}$$

Also, there exists an addition theorem for spherical harmonics

$$\sum_{m=-\ell} Y_\ell^{*m}(\theta,\phi) Y_\ell^m(\theta'.\phi') = \left(\frac{2\ell+1}{4\pi}\right)^{1/2} Y_\ell^0(\alpha). \tag{B.5}$$

The wave function of a plane wave with wave number k propagating along the z axis can be described by

$$\mathrm{e}^{ikz} = \mathrm{e}^{ikr\cos(\theta)} \tag{B.6}$$

$$= \sum_{\ell=0}^{\infty} A_\ell(r) Y_{\ell,0}(\theta), \tag{B.7}$$

where

$$A_\ell(r) = \int \mathrm{d}\Omega\, Y_{\ell,0}^*(\theta)\mathrm{e}^{ikr\cos(\theta)} = i^\ell\sqrt{4\pi(2\ell+1)}\, j_\ell(kr), \tag{B.8}$$

where the last equality shows the coefficient $A_\ell(r)$ can be expressed in terms of a spherical Bessel function $j_\ell(kr)$. Using the addition theorem equation (B.6) yields the decomposition of a plane wave into spherical Bessel functions

$$e^{i\mathbf{k}\cdot\mathbf{r}} = 4\pi \sum_{\ell,m} i^\ell j_\ell(kr) Y_\ell^{m*}(\theta,\phi) Y_\ell^m(\theta,\phi) \tag{B.9}$$

B.2 Hankel transform

B.3 Coulomb wave functions

The Coulomb wave equation for a charged particle with arbitrary angular momentum and charge is given by

$$\nabla^2\psi + \left(k^2 - \frac{2\mu}{\hbar^2}V(r)\right)\psi = 0, \tag{B.10}$$

where μ is the reduced mass of the system. The radial wave function $u(r)$ satisfied the following differential equation

$$\frac{d^2u_\ell}{dr^2} + \left(k^2 - \frac{\ell(\ell+1)}{r^2} - \frac{2\mu}{\hbar^2}\frac{Ze^2}{r}\right)u_\ell = 0, \tag{B.11}$$

where Z is the product of the charges. Two independent solutions can be found to equation (B.11) – these are called the regular and irregular Coulomb wave functions denoted $F_\ell(r)$ and $G_\ell(r)$ respectively. The regular Coulomb wave function $F_\ell(r)$ is a real function that vanishes at $r = 0$ and the behaviour of the function is described using a parameter η which describes how strongly the Coulomb interaction is

$$\eta = \frac{Zmc\alpha}{\hbar k}, \tag{B.12}$$

where m is the mass of the particle, k is the wave number and α is the fine structure constant. The solution to is given by

$$F_\ell(\eta, kr) = C_\ell(\eta)(kr)^{\ell+1}e^{-ikr}{}_1F_1(\ell+1-i\eta, 2\ell+2, 2ikr), \tag{B.13}$$

where ${}_1F_1(kr)$ is a confluent hypergeometric function and $C_\ell(\eta)$ is a normalization constant given by

$$C_\ell(\eta) = \frac{2^\ell e^{-\pi\eta/2}\left|\Gamma(\ell+1+i\eta)\right|}{(2\ell+1)!}, \tag{B.14}$$

where Γ is the gamma function. For numerical purposes, it is useful to use the integral representation of equation (B.13) [4, eq. 33.7.1]

$$F_\ell(\eta,\rho) = \frac{\rho^{\ell+1}2^\ell e^{i\rho-(\pi\eta/2)}}{|\Gamma(\ell+1+i\eta)|}\int_0^1 e^{-2i\rho t}t^{\ell+i\eta}(1-t)^{\ell-i\eta}\,dt. \tag{B.15}$$

For particles without charge, we can ignore the Coulomb interaction in equation (B.11) and the solution becomes [2]

$$F_\ell(kr) = \left(\frac{\pi kr}{2}\right)^{1/2} J_{\ell+1/2}(kr), \quad \text{particles without charge} \tag{B.16}$$

where $J_{\ell+1/2}$ is a Bessel function. Equation (B.16) is nothing but a spherical Bessel function. This means in the limit where the particles become chargeless the solution must reduce to a plane wave solution.

Appendix C

Three component wavefunction

Strictly speaking, the nuclear model should be consistent with other results from nuclear physics. In particular, the mass difference between the charged pion and the neutral pion. A priori we do not know the impact on the wave function of the nucleon-pion system and in this appendix, we wish to estimate how the wave function changes when we take the different properties of the pion into account. Starting from (3.15) and (3.16)

$$\psi_p = p\uparrow\frac{1}{\sqrt{V}}, \quad \psi_{N\pi^0} = (\boldsymbol{\tau}\cdot\boldsymbol{\pi})(\boldsymbol{\sigma}\cdot\mathbf{r})\phi_0(r)p\uparrow\frac{1}{\sqrt{V}}, \quad \psi_{N\pi^+} = (\boldsymbol{\tau}\cdot\boldsymbol{\pi})(\boldsymbol{\sigma}\cdot\mathbf{r})\phi_+(r)p\uparrow\frac{1}{\sqrt{V}}, \tag{C.1}$$

and these will act as the state vector in our system. Constructing a similar Hamiltonian for the three-component wave function yields

$$\begin{bmatrix} K_{\mathbf{p}} & W^\dagger & W^\dagger \\ W & K_{\mathbf{p}} + K_0 + m_{\pi^0} & 0 \\ W & 0 & K_{\mathbf{p}} + K_+ + m_{\pi^+} \end{bmatrix} \begin{bmatrix} \psi_p \\ \psi_{N\pi^0} \\ \psi_{N\pi^+} \end{bmatrix} = E \begin{bmatrix} \psi_p \\ \psi_{N\pi^0} \\ \psi_{N\pi^+} \end{bmatrix}, \tag{C.2}$$

where K_i is the kinetic operator and W, $W^\dagger$ are the creation and annihilation of a pion respectively. This leads to three coupled equations

$$W^\dagger\psi_{N\pi^0} + W^\dagger\psi_{N\pi^+} = E\psi_p \tag{C.3}$$

$$W\psi_p + (K_0 + m_{\pi^0})\psi_{N\pi^0} = E\psi_{N\pi^0} \tag{C.4}$$

$$W\psi_p + (K_+ + m_{\pi^+})\psi_{N\pi^+} = E\psi_{N\pi^+}. \tag{C.5}$$

The calculations are completely analogous to what is done in chapter 3 and the final set of equations are given by

$$\left.\begin{aligned} 12\pi\int_0^\infty \mathrm{d}r\, f(r)\phi_0(r)r^4 + 12\pi\int_0^\infty \mathrm{d}r\, f(r)\phi_+(r)r^4 = E \\ f(r) - \frac{\hbar^2}{2\mu_0}\left(\frac{\mathrm{d}^2\phi_0(r)}{\mathrm{d}r^2} + \frac{4}{r}\frac{\mathrm{d}\phi_0(r)}{\mathrm{d}r}\right) + m_\pi^0 c^2\phi_0(r) = E\phi_0(r) \\ f(r) - \frac{\hbar^2}{2\mu_+}\left(\frac{\mathrm{d}^2\phi_+(r)}{\mathrm{d}r^2} + \frac{4}{r}\frac{\mathrm{d}\phi_+(r)}{\mathrm{d}r}\right) + m_\pi^+ c^2\phi_+(r) = E\phi_+(r) \end{aligned}\right\} \tag{C.6}$$

Physically, we have added another pion wave function to our original model yet it is still bound by the total energy of the system, E. Numerically this is almost the same system and the solutions can be found using the same numerical considerations as in section 3.4. The results are shown in C.1

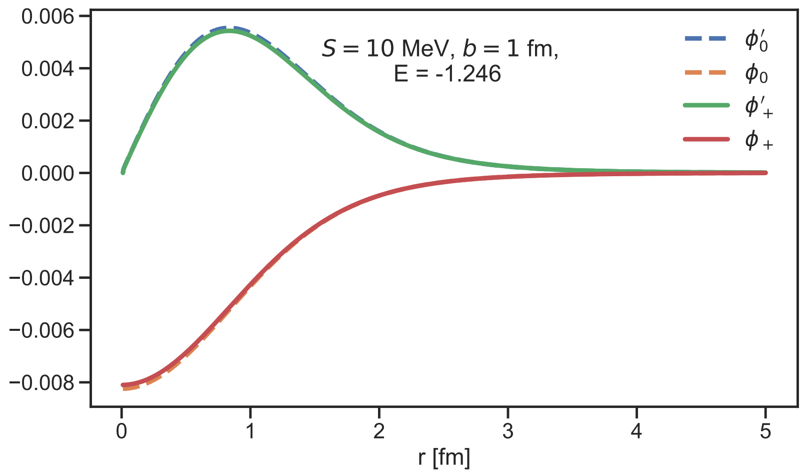

Figure C.1: Solutions to (C.6). The difference in the wave function is minimal compared to the two-component wave function. The energy is approximately equal to the sum of the two individual systems.

Compared to 3.4 the difference is negligible even accounting for the mass difference for the pions and nucleons (m_N, m_P). This means we can to a good estimation continue using only one pion wave function in our nuclear model.

Appendix D

Angular distribution

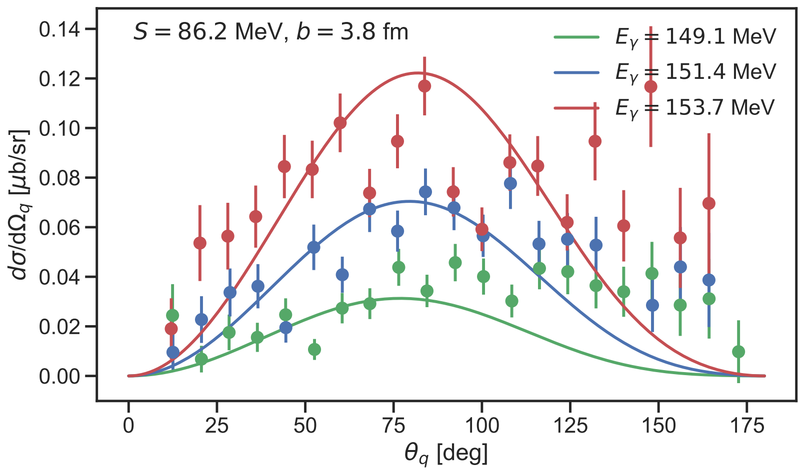

Figure D.1: Angular distribution with the parameters $S = 86.2$ MeV and $b = 3.8$ fm using the relativistic density of states

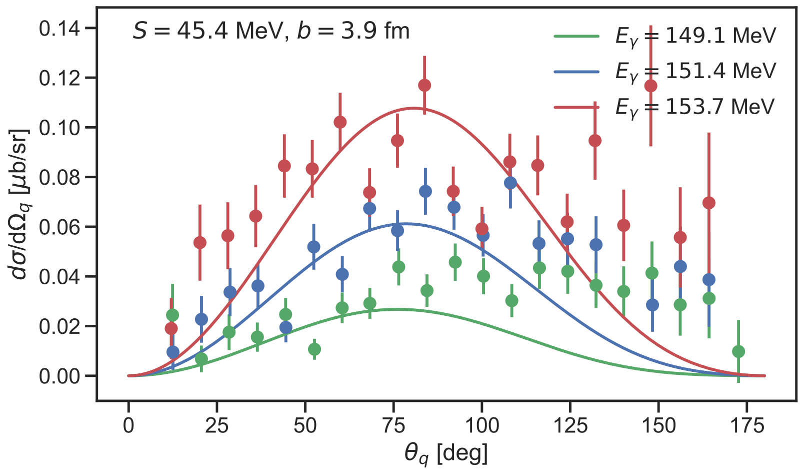

Figure D.2: Angular distribution with the parameters $S = 45.4$ MeV and $b = 3.9$ fm using the relativistic density of state

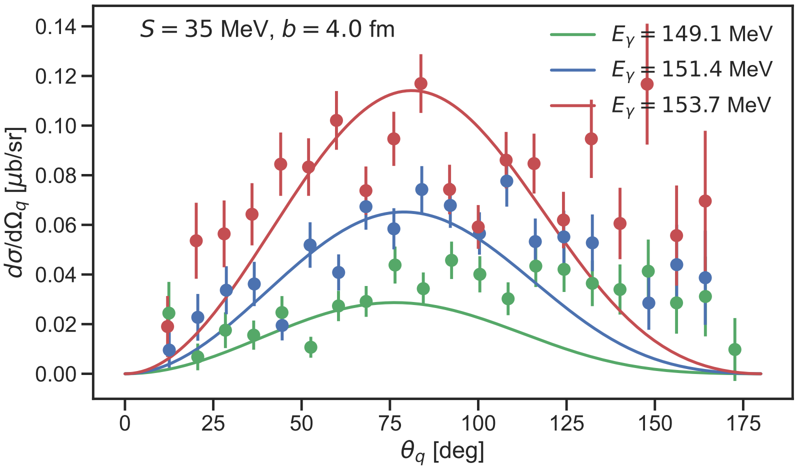

Figure D.3: Angular distribution with the parameters $S = 35$ MeV and $b = 4.0$ fm using the relativistic density of state

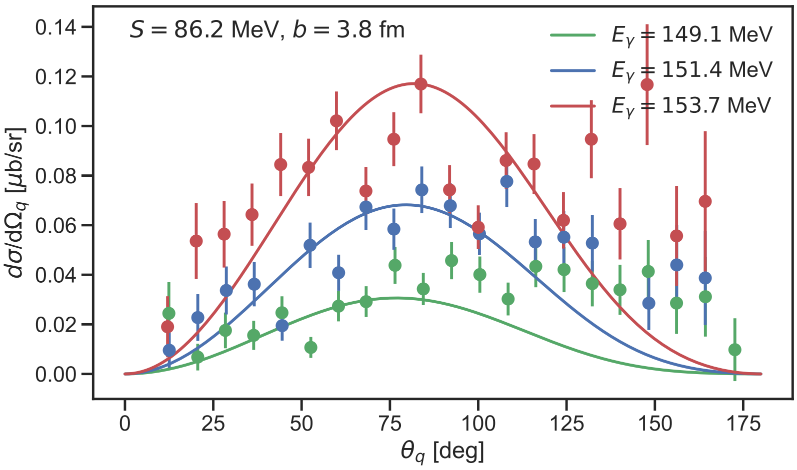

Figure D.4: Angular distribution with the parameters $S = 86.2$ MeV and $b = 3.8$ fm using the non-relativistic density of states

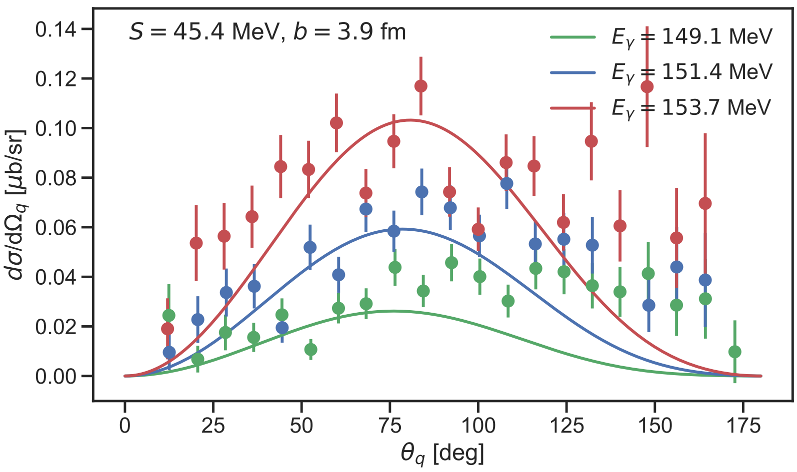

Figure D.5: Angular distribution with the parameters $S = 45.4$ MeV and $b = 3.9$ fm using the non-relativistic density of state

Figure D.6: Angular distribution with the parameters $S = 35$ MeV and $b = 4.0$ fm using the non-relativistic density of state